Talanta Open 13 (2026) 100615

Contents lists available at ScienceDirect

Talanta Open

journal homepage: www.sciencedirect.com/journal/talanta-open

Microplastics and Nanoplastics in human tissues: Systematic review of evidence, analytical protocols, and methodological challenges

Simone Ottavio Zielli [a,b], Jennifer Paola Pascali [b], Antonio Mazzotti [a,c,*], Paolo Fais [b], Milena Fini [d], Cesare Faldini [a,c], Susi Pelotti [b]

[a] IRCCS Istituto Ortopedico Rizzoli, 1st Orthopaedic and Traumatologic Clinic, Via Giulio Cesare Pupilli 1, Bologna, 40136, Italy
[b] Department of Medical and Surgical Sciences, Unit of Legal Medicine, University of Bologna, Via Irnerio 49, Bologna, 40126, Italy
[c] Department of Biomedical and Neuromotor Science-DIBINEM, University of Bologna, Bologna, 40136, Italy
[d] IRCCS Istituto Ortopedico Rizzoli, Via di Barbiano, Scientific Direction, 1/10, 40136 Bologna, Italy

ARTICLE INFO

Keywords:
Microplastics
Human tissues
Raman spectroscopy
FTIR spectroscopy
Chemical digestion
Contamination control

ABSTRACT

Microplastics and NanoPlastics (MNP) have emerged as ubiquitous environmental contaminants with potential implications for human health. This systematic review synthesizes current evidence on the occurrence of MNP in human solid tissues and critically evaluates the analytical protocols employed for their detection and quantification. A comprehensive literature search conducted in September 2025 across MEDLINE, EMBASE, and the Cochrane Library, in accordance with PRISMA guidelines, identified 26 eligible studies encompassing 564 human samples from diverse biological matrices, including placenta, lung, liver, blood, and bone.

Polyethylene, polypropylene, and polyvinyl chloride were the most frequently detected polymers, while particle sizes predominantly ranged between 20 and 100 μm. Analytical techniques varied substantially across studies, with Raman and Fourier-transform infrared (FTIR) spectroscopy representing the most widely applied methods, often complemented by microscopy or pyrolysis–GC/MS for polymer confirmation. Reported MNPs abundances ranged from less than one to several thousand particles per gram of tissue, reflecting the lack of standardized procedures for extraction, quantification, and contamination control.

Recent investigations have increasingly implemented plastic-free workflows and procedural blanks, leading to improved reliability and reduced overestimation of MNP burden. Nevertheless, persistent methodological heterogeneity continues to hinder cross-study comparability and the establishment of true human tissue loads. Preliminary correlations between MNP accumulation and clinical or pathological parameters have been observed, but causal links remain unconfirmed.

This review highlights the urgent need for internationally harmonized protocols, rigorous contamination prevention, and standardized reporting to ensure reliable biomonitoring and clarify the potential health implications of microplastic exposure in humans.

1. Introduction

In 2023, 400.3 million metric tons of plastic were produced globally, reflecting the massive scale of plastic production and its pervasive presence in modern life [1]. Plastics, or polymers, are materials primarily composed of large chemical compounds produced through industrial polymerization processes, forming an extensive and varied category of substances [2].

Microplastics are defined as any water-insoluble synthetic solid particles or polymer matrices of primary or secondary origin, with sizes ranging from 1 μm to 5 mm, regardless of their shape [3–6]. Nanoplastics, although less precisely defined, typically refer to plastic particles smaller than 1 μm, resulting from further fragmentation [7]. Micro and NanoPlastics (MNPs) can be classified into primary (manufactured particles, such as pre-production pellets, abrasion particles, such as microbeads in cosmetics) and secondary particles derived from predominantly UV-induced and mechanical degradation of larger plastic pieces.

The biodegradability of plastics is influenced by the raw materials, their chemical composition and structure, and environmental conditions

* Corresponding author at: 1st orthopaedic and Traumatology Clinic, Istituto Ortopedico Rizzoli, 40136 Bologna, Italy
E-mail addresses: antonio.mazzotti@ior.it (A. Mazzotti), milena.fini@ior.it (M. Fini).

https://doi.org/10.1016/j.talo.2026.100615
Received 18 November 2025; Received in revised form 5 January 2026; Accepted 10 January 2026
Available online 16 January 2026

such as sunlight, water, wind, and biological processes [8–10].

Plastic pollution poses a significant global challenge due to its ubiquitous use. Exposure to micro- and nano-plastics (MNPs) occurs not only directly, due to their wide dissemination in everyday consumer goods and high abundance in the environment, but also indirectly through the food chain. These particles are easily ingested by living organisms and undergo continuous bioaccumulation and biomagnification [11,12]. The detection of MNPs in remote regions indicates atmospheric transport as a significant means of global dissemination, presenting a potential global health risk. The European Union (EU) aims to reduce MNPs releases by 30 % by 2030 [13], focusing on restricting the use of intentionally added MNPs in products and minimizing unintentional microplastic releases. Currently, no comprehensive EU legislation specifically addresses MPs. However, partial objectives are covered by the European Chemical Agency (REACH) restriction proposal, which targets intentionally added MPs, which unfortunately regards the 5 % of total plastic.

Human exposure to MNPs has been confirmed through various studies and methods [14,15]. An increasing number of studies have highlighted the presence of MNPs at various levels within the human body [16]. MNPs have been found in different biological fluids [17–20], throughout the gastrointestinal tract and the respiratory system [21–24]. Additionally, research has expanded to intuitively less exposed tissues, such as venous tissue, and synovia [25,26].

The abundance of MNPs in the environment justifies their presence in biological fluids to some extent. However, ongoing research aims to investigate the potential effects these environmental pollutants have at the tissue level, with significant pathological implications.

Some potential effects have already been described. Notably, MNPs presence in the reproductive system has been correlated with delays in gestational age and adverse birth outcomes [17]. Additionally, at the gastrointestinal level, MNPs have been shown to contribute to gallstone formation and have observed effects on the intestinal microbiota [21]. The mechanisms underlying the toxicity of these pollutants are still being explored, both in vivo and in-vitro studies [27–30]. Authors have demonstrated different pathological actions, such as triggering premature cellular senescence in endothelial and neuronal cells [28,29].

The presence of MNPs in such a wide range of tissues and their potential pathogenic roles in the human body has led to an exponential increase in research. However, the methods used for samples identification, procession and quantification of MNPs are often disparate, as there is currently no gold standard. Additionally, there is a lack of standardized protocols for MNPs extraction, sample processing or even for the plastic-free protocols to prevent any contamination from commonly used plastic laboratory tools.

The aim of this systematic review was to identify which human solid tissues have been shown to contain MNPs and to provide a comprehensive overview of the analytical protocols developed for their detection and characterization. By comparing methodological approaches and assessing current limitations in standardization and contamination control, this review seeks to bridge existing knowledge gaps and lay the groundwork for more reliable and reproducible MNPs analysis in human tissues.

2. Materials and methods

In September 2025, a systematic review of the MEDLINE, EMBASE, and Cochrane Library databases was performed based on the Preferred Reporting Items for Systematic Reviews and Meta-Analyses (PRISMA) guidelines.

The search terms used were: “Microplastics” OR “Nanoplastics” AND “Human”.

Studies were included if they met the following criteria:

(1) peer-reviewed original articles,
(2) research conducted on human subjects, and
(3) analysis of solid biological tissues for the detection or characterization of microplastics (MPs) or nanoplastics (NPs).

Exclusion criteria were:

(1) case reports, narrative reviews, or commentaries;
(2) studies on non-human models or in vitro systems; and
(3) papers lacking methodological details on MNPs isolation or identification.

All duplicates were removed prior to screening. Two independent reviewers screened titles, abstracts, and full-texts, and any discrepancies were resolved through discussion with a senior author. A manual search of reference lists from the included studies was also performed to identify additional eligible publications.

2.1. Number of samples

For each study, data on the number and type of analysed samples were extracted, along with available participant demographics (e.g., age, sex, and health status). When provided, the distinction between pathological and control tissues was recorded.

2.2. Sample collection

Information regarding sample acquisition procedures was extracted, including details on tissue handling during surgery or autopsy, storage conditions, and measures taken to prevent plastic contamination.

Precautions such as the use of metal or glass instruments, cotton laboratory apparel, or filtered reagents were recorded where available.

2.3. Extraction of microplastics

Detailed descriptions of digestion and separation protocols were reviewed to assess methodological variability among studies. The chemical reagents employed (e.g., hydrogen peroxide, nitric acid, or enzymatic solutions), filtration media, and sample processing equipment were recorded. When specified, storage and preservation methods prior to analysis were also noted, given their relevance for maintaining polymer integrity.

2.4. MNPs detection and identification techniques

Analytical methods used for MNPs detection and polymer identification were extracted and categorized according to the main approach employed—spectroscopic (FTIR, Raman, LD-IR), microscopic (optical, SEM/EDS), or thermochemical (Py-GC/MS).

Where reported, details regarding spectral libraries, particle size thresholds, and validation procedures (e.g., comparison with polymer standards) were included.

2.5. Procedural blanks and negative controls

To assess methodological rigor, each study was evaluated for the inclusion of procedural blanks, laboratory blanks, or negative controls designed to detect background contamination.

Information on the type of blank employed (e.g., reagent-only controls, air exposure membranes, accompanying tissue blanks) and blank correction methods (subtraction, LOD/LOQ adjustment) was systematically collected.

2.6. Polymer composition and microplastic abundance

For each study, qualitative polymer identification and quantitative results were extracted, expressed as particles per gram, μg/g, or relative abundance. Additional characteristics—such as particle morphology,

color, and size distribution—were recorded when available. Data were synthesized to highlight inter-study variability in both polymer profiles and MNPs concentrations across different human tissues through a tabular comparaison.

3. Results

A total of 26 studies published between January 2020 and September 2025 were included. PRISMA flow chart is illustrated in Fig. 1.

3.1. Sample size and demographics

Across the 26 studies included in this review, a total of 564 human samples were analysed, covering a wide spectrum of biological matrices such as blood, placenta, liver, kidney, lung, colon, bone, cartilage, synovia, testis, and penile tissue. Sample sizes ranged from single case reports to large clinical or biobank-derived cohorts (up to 100 participants). The age of individuals spanned from 16 to 88 years, encompassing both sexes and diverse health conditions. Participants included healthy volunteers, patients undergoing surgical procedures for vascular, oncological, or inflammatory diseases, and post-mortem donors collected through medico-legal or neuropathological autopsies.

Approximately half of the analysed cohorts consisted of pregnant women, primarily with uncomplicated or low-risk pregnancies, allowing assessment of microplastic presence in placental and umbilical tissues. The remaining studies investigated subjects with defined clinical backgrounds, including carotid artery stenosis, Crohn's disease, colorectal cancer, hematological malignancies, and penile cancer, among others. This heterogeneity in sample type and participant demographics reflects the growing multidisciplinary effort to characterize microplastic distribution across distinct human organ systems and physiological contexts, from gestational to post-mortem conditions (Table 1).

3.2. MNPs collection

Sample collection procedures varied according to tissue type and study design but were generally characterized by strict contamination control measures. Most human tissues were obtained either during surgical procedures, autopsies, or post-mortem examinations, and were immediately stored in pre-cleaned glass containers at −80 °C or in formalin. Across studies, a strong emphasis was placed on plastic-free workflows, with nearly all authors employing glass or metal instruments, cotton laboratory garments, and filtered reagents (typically < 0.45 μm).

To minimize environmental contamination, laminar flow cabinets, ISO-class clean environments, and procedural blanks were routinely

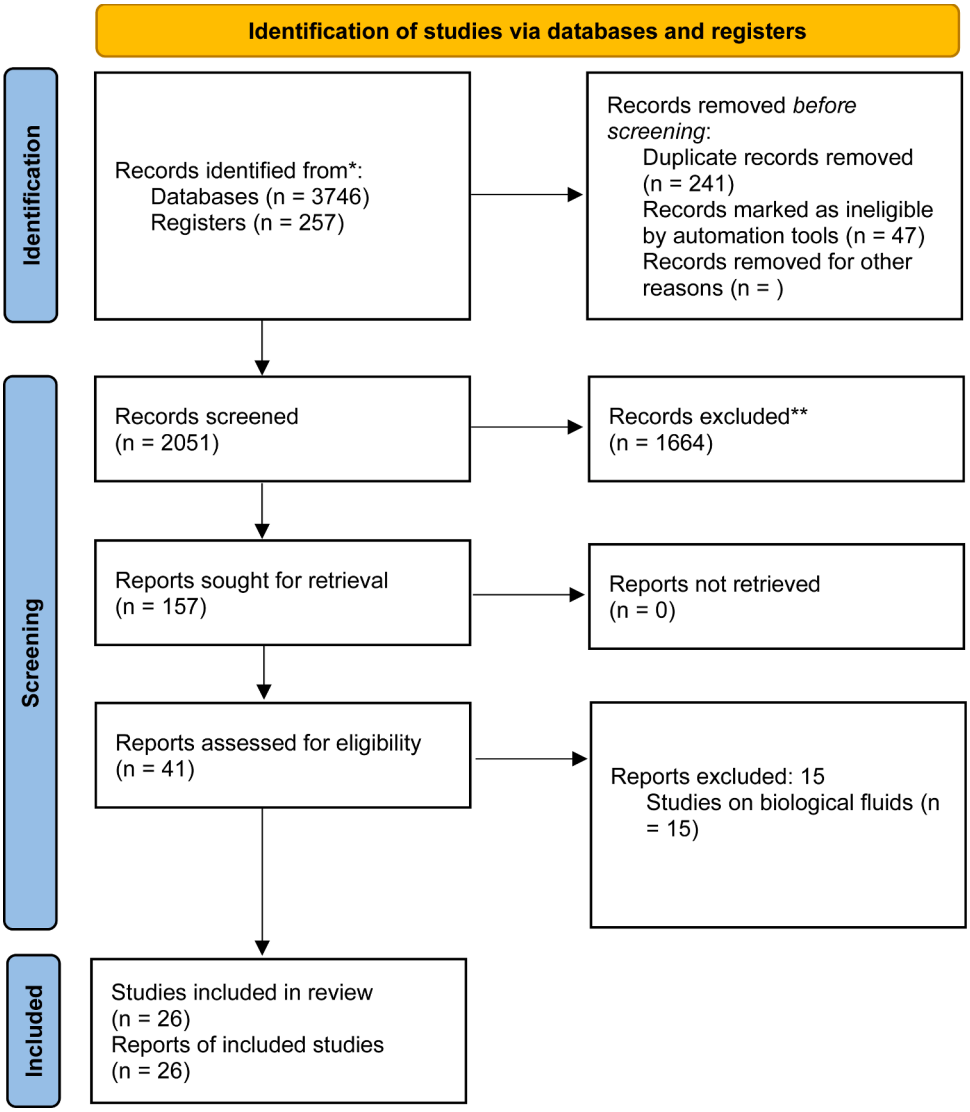

Fig. 1. PRISMA 2020 flow diagram for new systematic reviews which included searches of databases and registers only.

Table 1
Summary of included studies reporting microplastic detection in human tissues.

Author	Sample Size	Age (years)	Tissue	Health Status
Cui, 2025 [31]	20	Mean 66 ± 7; 60 % male	Blood, carotid plaques	Carotid artery stenosis ≥70 %; comorbidities: hypertension 60 %, diabetes 25 %, prior stroke 60 %
Codrington, 2024 [32]	6	Adult men ≥18 (mean N/R)	Penile corpus tissue	Erectile dysfunction; undergoing multi-component IPP surgery
Dzierżyński, 2025 [33]	1 (post-mortem)	24	Brain (white matter), thyroid, kidney, liver, muscle, heart, lung	Healthy; death by suicide; no prior hospitalization
Wu, 2025 [34]	32 (10 patients)	Median 29.5; BMI 17.6	Ileum (strictured/ non-strictured), mesenteric adipose (CF, CD-MAT)	Crohn's disease with intestinal fibrosis and inflammation
Garcia, 2024 [35]	81	N/R	Placenta (villous parenchyma; membranes removed)	Healthy pregnancies
Hu, 2024 [36]	23	16–88	Testis	Adult deceased individuals; medico-legal collection
Zhang, 2025 [37]	48	N/R	Endometrial tissue (~0.5 g); urine (2 mL)	Healthy pregnancies
Wang, 2025 [38]	17	Mean 58.1	Penile tissue (cancerous and adjacent non-cancerous)	Penile cancer; comorbidities: hypertension 8, diabetes 4; smokers 8, alcohol 9
Wanderley Lopes de Oliveira, 2025 [39]	10	Mean 26.7 ± 5.1	Placenta (50 g) and umbilical cord (50 g)	Healthy pregnancies; no autoimmune/ genetic disorders; gestational age 38.3 ± 1.1 weeks
Sun, 2024 [40]	12	7 patients <35 (58.3 %), 5 patients ≥35 (41.7 %)	Placenta, umbilical cord, fetal membrane	Healthy pregnancies; exclusion of chronic, autoimmune, genetic diseases
Pan, 2025 [41]	20 (10 patients)	Mean 69.9 ± 9.1	Colorectal tumor and adjacent tissue (≥5 cm)	Stage I–IV colorectal cancer; no other malignancies or chronic diseases
Guo, 2024 [42]	21	Median 56 (range 16–68)	Bone marrow	Hematological tumors (AML, pH+ MPAL, AMoL, APL)
Yang, 2025 [43]	16	Median 62.8 (range 38–83)	Bone, cartilage, intervertebral disc	Clinical volunteers; no malignancy/ systemic disease reported
Nihart, 2024 [44]	>90	Mean 36.6–84.0 (by cohort)	Liver, kidney, frontal cortex (brain)	Autopsy and brain bank donors; natural, traumatic, or substance-related deaths; dementia/ normal controls
Zhu, 2023 [45]	17	23–36	Placenta	Healthy pregnancies
Amereh, 2022 [46]	43	N/R	Placenta	Healthy pregnancies
Ragusa, 2022 [47]	30	N/R	Placenta	Low-risk single-fetus pregnancies
Ragusa, 2021 [48]	6	N/R	Placenta	Healthy pregnancies
Braun, 2021 [18]	2	N/R	Placenta	N/R
Chen, 2022 [49]	100	N/R	Lung	NSCLC patients undergoing VATS lobectomy/ sublobectomy
Jenner, 2022 [50]	13	Mean 63 ± 13 (32–77)	Lung	N/R
Amato-Lourenço, 2021 [22]	20	N/R	Lung	Non-smoking adults; routine coroner autopsy
Ibrahim, 2021 [24]	11	Mean 45.7	Colon	N/R
Horvatits, 2021 [23]	17	N/R	Liver, kidney, spleen	N/R
Rotchell, 2023 [25]	5	Mean 71.8 ± 2.5 (68–75)	Vein	N/R
Li, 2024 [26]	45	Mean 62.9 ± 11.1	Synovia	Patients undergoing lower-limb arthroplasty

Notes: MNPs = microplastics; N/R: Not reported in the original publication. Despite attempts to contact the corresponding authors, the missing information could not be retrieved and is therefore reported as a limitation of the available evidence.

used. Additionally, several studies included procedural blanks such as air and solvent controls, confirming the absence of exogenous MNPs prior to analysis (Table 2).

3.3. MNPs extraction

Extraction of MNPsfrom human tissues showed a marked heterogeneity among studies, underscoring the current lack of a standardized analytical framework. Nonetheless, several methodological patterns could be identified. Most investigations relied on alkaline digestion using potassium hydroxide (KOH, 5–10 %) at 40–60 °C for 24 h to 7 days, followed by filtration on glass fiber or stainless-steel membranes and subsequent spectroscopic or pyrolytic identification, including Raman, Laser Direct Infrared (LDIR), or Py-GC/MS techniques.

A subset of studies employed oxidative or acid digestion methods—typically using hydrogen peroxide (H_2O_2, 30 %) or concentrated nitric acid—to enhance tissue degradation, particularly for dense or fibrotic matrices. Notably, Pan (2025), Sun (2024), and Wang (2025) implemented nitric-acid–based protocols coupled with heating on graphite plates or under fume hood conditions, often followed by ultrasonic dispersion in ethanol to minimize particle aggregation.

More refined enzymatic and multi-step solvent-based approaches were also reported, aiming to preserve particle morphology and reduce polymer degradation. Cui (2025) adopted enzymatic digestion with proteinase K for both blood and plaque samples, while Amato-Lourenço (2021) combined Corolase® 7089 enzymatic treatment with density separation using $ZnCl_2$, improving polymer recovery efficiency.

Among the most complex methods, Dzierżyński (2025) applied a two-week oxidative digestion with 30 % H_2O_2, followed by vacuum

Table 2
Overview of sample collection procedures and contamination control measures.

Author	Sample Collection Methods	Precautions Against Contamination
Cui, 2025 [31]	Blood: 10 mL pre-surgery in glass tubes (for MPs) and EDTA-coated plastic tubes (for lipids). Plaques surgically excised, rinsed with PBS, snap-frozen, stored at −80 °C in MPs-free amber glass vials	Laminar flow hood; glass/stainless-steel instruments rinsed with 0.22 μm ultrapure water; cotton lab coats and nitrile gloves; field/procedural blanks;
Codrington, 2024 [32]	Tissue retrieved from corpora with stainless steel forceps before corporotomy; stored in 25 mL glass Erlenmeyer flasks with glass stoppers. One control sample collected in polypropylene container	Class 100 clean benches; filtration of all reagents with 0.4 μm PC membranes; only glass/metal labware used; glassware cleaned with Milli-Q water, ethanol, heated at 250 °C for 8 h; procedural blanks included
Dzierżyński, 2025 [33]	Post-mortem autopsy 24 h after death; tissue collected with ceramic instruments, rinsed with ultrapure water; stored in acid-washed glass Petri dishes; frozen at −80 °C	All solutions filtered through 0.1 μm PTFE membranes; use of cotton gowns, masks, gloves; ceramic tools; ultrapure water (18.2 MΩ·cm); acid-washed glassware; procedural blanks and controls analyzed in parallel
Wu, 2025 [34]	Ileum and mesenteric adipose collected (1 × 1 × 1 cm^3) during surgical resection; transferred into sterile glass containers with wooden lids; processed within 24 h	Solvents filtered <0.45 μm; only glassware used (rinsed with ethanol); stainless steel membranes tested with Raman to ensure MP-free; cotton gloves, non-plastic lab coats; blank controls with MilliQ water (no MNPs detected)
Garcia, 2024 [35]	Placental tissue cuboids excised 4 cm from cord insertion; decidua/amnion removed; immediately flash frozen at −80 °C; stored without thawing or re-aliquoting	Use of sterile glass vials; all digestion in glass; solvents handled under controlled conditions; blanks run in parallel; avoidance of maternal/fetal surface tissue to minimize contamination; cryovials and ultracentrifuge tubes tested for polymer background
Hu, 2024 [36]	Archived testicular tissue from New Mexico Office of the Medical Investigator, collected in 2016 and stored ≥7 years before release	Standard lab precautions; ultracentrifugation to separate MPs; protocols referenced from Garcia et al., 2024
Zhang, 2025 [37]	Endometrial tissue collected at delivery; urine samples collected concurrently	ISO Class 5 clean environments; cotton-only clothing; pre-combusted glassware; glass containers & filters; blanks and environmental controls
Wang, 2025 [38]	Samples collected in laminar-flow operating room; surgical staff in sterile cotton gowns, nitrile gloves, masks; tissues retrieved with stainless steel forceps, stored in glass containers	Plastic-free protocol; sterile cotton clothing, particle-free nitrile gloves; ethanol-cleaned benches; glassware rinsed with filtered deionized water; blanks and Milli-Q water controls showed no contamination
Wanderley Lopes de Oliveira, 2025 [39]	Samples collected at delivery (cesarean or vaginal) at HUPAA–UFAL hospital; placed in glass containers with stainless steel lids	Strict plastic-free protocol; all glass or metal materials; controls for air, Milli-Q, PBS, and KOH exposure; detected airborne MNPs excluded from analysis
Sun, 2024 [40]	Samples collected during cesarean section; placenta (maternal surface near cord attachment), umbilical cord (3 g), and fetal membrane; placed in pre-cleaned glass bottles and stored at −80 °C	Entire procedure plastic-free: all glass or metal tools; cotton drapes; nitrile gloves; activated carbon masks; procedural and air blanks confirmed free of MNPs (>80 % match criterion)
Pan, 2025 [41]	Tissue collected intraoperatively during tumor resection; immediately stored at −80 °C in sterile glass containers	Use of all-glass consumables; solvents filtered through 0.45 μm PTFE membranes; blanks (reagent, solvent, lab); use of anti-static clothing, gloves, dust-free workspace; external QC plan
Guo, 2024 [42]	3–5 mL bone marrow aspirated under local anesthesia in lateral decubitus; collected in EDTA anticoagulant tubes by clinicians at Henan Cancer Hospital	Plastic-free workflow; all-glassware; cotton lab coats, nitrile gloves; reagents filtered (0.45 μm PTFE); procedural blanks with MilliQ water; recovery 81.6–117.4 %
Yang, 2025 [43]	Human skeletal tissues collected during orthopedic surgery; immediately stored and prepared for microplastic analysis	Plastic-free procedures; glass and metal instruments; contamination checks not detailed but consistent with prior microplastic protocols
Nihart, 2024 [44]	Collected fresh during autopsy (NM OMI) or post-mortem (brain banks). Organs dissected under refrigeration; liver section from right central parenchyma, kidney wedge (cortex + medulla), brain: frontal cortex or anterior prefrontal cortex. Stored in 10 % or 20 % formalin or frozen.	Stainless steel dissection instruments; polyethylene cutting boards; in-house prepared formalin; consistent autopsy environment since 2013; potential contamination from cutting boards and plastic jars acknowledged; identical collection procedures across years.
Zhu, 2023 [45]	Portions of the whole placentas were placed into clean glass bottles.	Plastic-free protocol strictly implemented; no plastic equipment used.
Amereh, 2022 [46]	Fresh placentas were deposited into a metal container and stored in glass bottles.	Plastic-free protocol; cotton gloves with inner rubber gloves; prewashed cotton towels used.
Ragusa, 2022 [47]	N/R	Plastic-free kit and protocol used.
Ragusa, 2021 [48]	N/R	Procedural blanks used to monitor and correct contamination.
Braun, 2021 [18]	Placenta tissues were sampled; meconium collected and transferred to glass bottles; biopsies cut and transferred to glass bottles.	Negative controls; contamination controls; materials rinsed with ultra-pure water, covered with aluminium foil, nitrile gloves worn.
Chen, 2022 [49]	Lung tissues transferred to 50-mL glass bottles.	All glassware cleaned and rinsed with Milli-Q water, covered with clean dust-free paper and aluminium foil.
Jenner, 2022 [50]	Tissue samples placed into empty glass containers with foil lids.	N/R
Amato-Lourenço, 2021 [22]	Samples processed in a clean laminar flow cabinet.	Materials washed with Milli-Q® water, nitric acid solution for glass materials, covered with aluminium foil, cotton coats and nitrile gloves used, procedural blanks, and control samples from stillborns.
Ibrahim, 2021 [24]	Tissue samples placed in formalin, one on filter paper in a glass Petri dish.	Formalin and filter paper checked for MNPS contamination.
Horvatits, 2021 [23]	Tissue samples weighed and transferred to glass beakers.	Clean environment and materials, pre-cleaning, sample covering, solution pre-filtration, blank samples analyzed.
Rotchell, 2023 [25]	Tissue samples placed into empty glass containers with	N/R

(*continued on next page*)

Table 2 (*continued*)

Author	Sample Collection Methods	Precautions Against Contamination
	foil lids, transported on ice, digested same day.	
Li, 2024 [26]	Specimens collected into glass bottles.	N/R

Notes - Abbreviations:.
N/R: Not reported in the original publication. Despite attempts to contact the corresponding authors, the missing information could not be retrieved and is therefore reported as a limitation of the available evidence. MNPs – Microplastics.
ABS – Acrylonitrile Butadiene Styrene *(only if referenced elsewhere in table series)*.
EDTA – Ethylenediaminetetraacetic Acid.
HUPAA–UFAL – Hospital Universitário Professor Alberto Antunes, Universidade Federal de Alagoas.
ISO – International Organization for Standardization.
KOH – Potassium Hydroxide.
LD-IR – Laser Direct Infrared Imaging *(if used across tables for consistency)*.
NM OMI – New Mexico Office of the Medical Investigator.
PBS – Phosphate-Buffered Saline.
PC – Polycarbonate.
PMMA – Polymethyl Methacrylate *(if referenced elsewhere)*.
PTFE – Polytetrafluoroethylene.
PVC – Polyvinyl Chloride.
QC – Quality Control.
SBR – Styrene–Butadiene Rubber.
SEM – Scanning Electron Microscopy *(for cross-table consistency)*.
µm – Micrometer (Micron).

filtration on aluminum oxide membranes (0.02 µm) and extensive multi-instrument characterization (FIB-SEM, O-PTIR, MALDI-TOF MS). Conversely, Guo (2024) utilized a high-temperature multi-solvent extraction to selectively dissolve and identify polymer classes (PA, PET, PP, PE) using Py-GC/MS and LDIR.

Overall, the reviewed evidence indicates a progressive convergence toward plastic-free, chemically controlled digestion and metal-based filtration protocols. However, substantial variability remains in reagents, incubation conditions, and downstream analytical techniques, emphasizing the absence of an internationally standardized methodology for MNPs isolation and quantification in human tissues (Table 3).

3.4. Identification and quantification of MPs

MNPs were consistently detected across all examined human tissues and biological matrices, though with marked inter-study variability in both abundance and polymeric composition. Reported burdens ranged from <1 particle/g in placental or intestinal samples to several thousand µg/g in neural or atherosclerotic tissues. The most frequently identified polymers were PE, PP, and PVC, followed by PET, PS, and PA, with occasional detection of technical polymers such as PU, PMMA, and POM in tumor or neural tissues. Particle dimensions were mainly within the 20–100 µm range, while some studies reported nanoscale aggregates.

Identification of MNPs was primarily achieved through FTIR and Raman microspectroscopy, either singly or in combination, often integrated with optical or electron microscopy for morphological assessment. LD-IR imaging [45] and SEM–EDS coupled with hot needle testing [24] represented alternative approaches, while Py-GC/MS was increasingly applied for polymer quantification and validation. Spectral matching was performed using dedicated libraries—commercial or in-house—with some authors applying baseline correction and vector normalization to improve spectral quality.

Filter membranes were manually examined under light microscopy to distinguish fibers and fragments, with imaging parameters optimized for a minimum spatial resolution of 0.5 µm. Several studies incorporated procedural blanks and laboratory controls to account for contamination and validate analytical accuracy, though their use remained inconsistent across investigations.

Correlations between MNPS abundance and biological or pathological parameters were occasionally observed—such as with fibrosis, lipid accumulation, or tumor grade—yet these associations remain preliminary and not universally reproducible [24,31,41] (Table 4).

3.5. Procedural blanks and negative controls

Procedural blanks and negative controls were included in the majority of studies to verify the absence of environmental contamination during tissue collection and sample processing. Out of all reviewed works, eighteen explicitly reported the use of procedural or blank controls, while two additional studies [46,51] implemented strict plastic-free protocols implying similar precautions. These controls typically consisted of reagent and solvent blanks, Milli-Q water checks, or air blanks, often accompanied by verification of laboratory materials through pyrolysis–GC/MS or spectroscopic screening. This systematic inclusion of contamination controls marks a progressive step toward methodological rigor, although the level of detail and implementation consistency remained variable across laboratories (Table 5).

3.6. Polymer composition and microplastic abundance

MNPs abundance and polymer composition varied widely between matrices and methodologies. Reported burdens ranged from <1 particle/g in placental samples to several thousand µg/g in brain and atherosclerotic tissues (Table 6).

The most frequently detected polymers were polyethylene (PE), polypropylene (PP), and polyvinyl chloride (PVC), in line with global production trends. PET, PS, and PA were also common, while technical polymers such as PU, PMMA, POM, or PTFE were occasionally reported in neural and tumor tissues, possibly reflecting healthcare or occupational exposure (Table 6).

Particles were mainly 20–100 µm in size, with smaller fragments or nanoscale aggregates detected in some studies. Fragments predominated over fibers, and colorless or white MNPs were most frequent. Concentrations tended to be higher in vascular and neural tissues, and some authors described associations with fibrosis, lipid accumulation, or reproductive parameters, though these findings remain preliminary (Table 6).

4. Discussion

The growing scientific attention toward MNPs contamination in humans is reflected by the marked increase in publications over the past four years. The 26 studies included in this review encompass a total of 564 human samples, spanning diverse tissues and health conditions. Among the analysed matrices, the placenta and lung tissue emerged as the most frequently examined, followed by hepatic, intestinal, and vascular samples—highlighting a predominant focus on organs that are either directly exposed to the environment or critically involved in metabolic exchange.

The particular attention to the placenta likely stems from both its biological vulnerability and its ethical and developmental implications. Detecting MNPs in this tissue raises essential questions regarding maternal–fetal transfer and potential developmental toxicity. Similarly, the high number of investigations on the respiratory and gastrointestinal systems reflects their roles as primary entry routes for airborne and dietary microplastics, respectively. This research trend aligns with clinical concerns linking chronic MNPs exposure with inflammation and carcinogenesis [49,52,53].

The analysed populations were markedly heterogeneous, ranging from healthy volunteers and obstetric cohorts to patients undergoing surgery for vascular, oncological, or orthopedic conditions, as well as post-mortem donors. This diversity illustrates an ongoing methodological shift—from purely descriptive detection studies toward more

Table 3
Overview of extraction methods, chemicals, and processing tools employed in MNPS analysis.

Author	Extraction Techniques	Chemical Reagents	Processing Equipment
Cui, 2025 [31]	Enzymatic digestion: blood with proteinase K (50 °C, 48 h); plaques homogenized, then same digestion; residues filtered and dried	Proteinase K, PBS	Sterile tissue grinder, pre-weighed glass fiber filters,
Codrington, 2024 [32]	Digestion with combined KOH, NaClO, Tween-20 solution; incubation at 45 °C (20 h) and 60 °C (4 h); filtration through PETG gold-coated membrane filters (0.8 μm pore size); dried and mounted for analysis	KOH, NaClO (13 %), Tween-20, Milli-Q water, ethanol	Stainless steel forceps, glass Erlenmeyer flasks, PETG filters, class 100 clean bench, LDIR (Agilent 8700), SEM (Zeiss Merlin), coating device (CCU-010)
Dzierżyński, 2025 [33]	Digestion in 30 % H_2O_2 at 50 °C under shaking (80 rpm) for ~2 weeks; vacuum filtration on aluminum oxide membrane filters (0.02 μm); filtrates lyophilized	H_2O_2, ultrapure water, tetrahydrofuran (THF), 1,8,9-anthracenetriol, Ag-TFA	Ceramic instruments, acid-washed glass Petri dishes, lyophilizer, aluminum oxide filters, FIB-SEM Scios 2, VHX-7000 microscope, mIRage O-PTIR system, Zetasizer Nano ZS, MALDI-TOF MS (Waters SYNAPT G2-Si HDMS)
Wu, 2025 [34]	Digestion with KOH (15 mL) at 60 °C for 3 h; vacuum filtration through 13 μm stainless steel membranes; rinsing with ultrapure water and ethanol; ultrasound dispersion; ethanol concentration to 150 μL; deposition on reflective glass slides for analysis	KOH solution, ethanol (99 %), ultrapure water, filtered solvents	Stainless steel membranes, ultrasonic bath, vacuum filtration system, infrared drying oven, highly reflective glass slides, Nikon SMZ 1000 microscope
Garcia, 2024 [35]	Alkaline digestion with 10 % KOH (3 × tissue volume), 40 °C, 72 h with agitation; ultracentrifugatio	10 % KOH solution (3 × tissue volume)	
Hu, 2024 [36]	Digestion + ultracentrifugation, followed by Py-GC–MS	KOH (from Garcia protocol), ethanol, polymer standards	Py-GC–MS (Agilent 6890 GC/5975 MS with Frontier EGA/PY-3030D), microbalance, stainless-steel Eco-cup SF
Zhang, 2025 [37]	Digestion with 10 % KOH at 60 °C for 24 h; filtration through sterile glass filters; drying overnight	KOH, polymer standards for Raman and Py-GC/MS calibration	Confocal Raman microscope (inVia™); Py-GC–MS (DB-5MS column, 600 °C pyrolysis)
Wang, 2025 [38]	Digestion with concentrated nitric acid (3 × volume of tissue); filtration (0.45 μm membrane); rinsing with anhydrous ethanol; ultrasonic treatment (0.5 h) to disperse particles	Nitric acid; ethanol (anhydrous); deionized water filtered through PTFE membranes	Agilent 8700 LDIR (laser direct infrared); fume hood conditions for prep
Wanderley Lopes de Oliveira, 2025 [39]	Digestion in 10 % KOH (1:9 w/v) at room teMNPs for 1 week; filtration through glass fiber filters (1.6 μm pores); rinsed with PBS and Milli-Q; air-dried	KOH, PBS, Milli-Q water	Optical microscopy (100 × Olympus IR); XploRA Micro-Raman Spectrometer (532 nm laser); KnowItAll + SLOPP/SLOPPe libraries
Sun, 2024 [40]	Digestion with triple-filtered nitric acid (3 × sample weight) for 48–72 h; concentration at 60 °C; vacuum filtration (stainless steel membrane, 13 μm pores); ethanol ultrasonic dispersion and drying	Nitric acid, ethanol (filtered 3 ×), ultrapure water	Agilent 8700 LDIR (Laser Direct Infrared Imaging); stainless steel vacuum filtration system
Pan, 2025 [41]	Tissue minced; digested in 68 % nitric acid (3 × sample volume) for 42 h at RT; additional 3 h on graphite heating plate; vacuum filtration (13 μm stainless steel membrane); ethanol ultrasonication; re-filtration and drying for LDIR	Concentrated nitric acid (68 %), ethanol, ultrapure water	Graphite heating plate; vacuum filtration system; IR drying oven (WA70–1); Agilent 8700 LDIR; Zeiss SEM
Guo, 2024 [42]	Multi-step solvent extraction: drying at 70 °C (4 h), sequential dissolution using hexafluoroisopropanol (PA66, PA6, PET), tetrahydrofuran (suspension adjustment), dichloromethane, and xylene (PP, PE) with ultrasonic extraction and heating at 150 °C	Hexafluoroisopropanol, tetrahydrofuran, dichloromethane, xylene, nitric acid, ethanol, ultrapure water	Py-GC/MS (Shimadzu QP2020NX, Frontier Lab PY3030D); Agilent 8700 LD-IR; SEM (Zeiss)
Yang, 2025 [43]	Digestion of tissue followed by chemical filtration and LD-IR detection; methodology adapted from previous validated microplastic extraction protocols	N/R in detail; nitric acid and ethanol likely; adapted from standardized tissue digestion protocols	LD-IR imaging spectrometer; SEM for morphology
Nihart, 2024 [44]	Tissue digestion via KOH followed by Py-GC/MS; benzene lipid removal step for improved polymer quantification; comparable methods across organs and timepoints.	KOH digestion, benzene (for lipid removal), formalin, ultrapure water	Pyrolysis–Gas Chromatography/Mass Spectrometry (Py-GC/MS); formalin-fixed tissue handling; analytical processing under controlled lab conditions.
Zhu, 2023 [45]	Samples digested using 10 % KOH in a 1:30 ratio of tissue to solution, incubated at 50 °C for 3 days. The digested material was filtered through a 10 μm stainless-steel membrane, followed by density separation using a potassium formate solution, ultrasonic treatment, and subsequent filtration.	10 % KOH, potassium formate solution, anhydrous ethanol	Glass beakers, stainless-steel membrane, ultrasonic bath, Erlenmeyer flask
Amereh, 2022 [46]	Samples digested in 10 % KOH (1:8 w/v) at room temperature for 7 days, filtered through Whatman No 47 filter paper.	10 % KOH	Glass containers, Whatman No 47 filter paper, glass Petri dishes
Ragusa, 2022 [47]	Samples collected and stored in glass containers at 0–7 °C. Samples fixed with glutaraldehyde in PBS and prepared using plastic-free procedures.	N/R	Metallic scalpel, glass containers
Ragusa, 2021 [48]	Samples digested in 10 % KOH (1:8 w/v) at room temperature for 7 days, filtered through 1.6 μm Whatman GF/A filter membrane.	10 % KOH	Glass containers, Whatman GF/A filter membrane, vacuum pump
Braun, 2021 [18]	Samples digested using NaOH (0.05 M) and then filtered through 50 μm stainless steel sieves, followed by filtration through 0.2 μm Anodisc membrane filter.	NaOH solution	Stainless steel sieve, Anodisc membrane filter, vacuum filtration system
Chen, 2022 [49]	Samples filtered through a 5-μm filter membrane after digestion.	N/R	5-μm filter membrane, glass Petri dishes
Jenner, 2022 [50]	Samples digested in 30 % H2O2, filtered onto aluminium oxide filters.	30 % H2O2	Glass conical flask, aluminium oxide filters, shaking incubator

(*continued on next page*)

Table 3 (*continued*)

Author	Extraction Techniques	Chemical Reagents	Processing Equipment
Amato-Lourenço, 2021 [22]	Samples digested using Corolase® 7089 enzyme, followed by density separation with ZnCl2 and filtration using silver membrane filters.	Corolase® 7089, ZnCl2	Silver membrane filters, oven
Ibrahim, 2021 [24]	Samples digested with 10 % KOH at 60 °C, diluted, and filtered using 0.45 μm cellulose membrane paper.	10 % KOH	Cellulose membrane paper, glass desiccator
Horvatits, 2021 [23]	Digestion with KOH and NaOCl, followed by filtration through silver membrane filters.	KOH, NaOCl, H2O2, acetone, ethanol	Silver membrane filters, beakers
Rotchell, 2023 [25]	Samples digested with triple-filtered H2O2, filtered onto aluminium oxide filters.	H2O2	Aluminium oxide filters, glass vacuum filtration system
Li, 2024 [26]	Samples digested with 30 % H2O2 at 65 °C, filtered onto mixed cellulose ester membrane filters.	30 % H2O2	Glass bottles, mixed cellulose ester membrane filters, vacuum-pumping system

Abbreviations:.
N/R – Not reported.
Ag-TFA – Silver Trifluoroacetate.
ATR-FTIR – Attenuated Total Reflectance Fourier Transform Infrared Spectroscopy *(if cross-referenced)*.
CCU – Compact Coating Unit.
FIB-SEM – Focused Ion Beam Scanning Electron Microscopy.
FTIR – Fourier Transform Infrared Spectroscopy.
GF/A – Glass Fiber Filter Type A.
H_2O_2 – Hydrogen Peroxide.
HDMS – High Definition Mass Spectrometry.
IR – Infrared.
KOH – Potassium Hydroxide.
LDIR – Laser Direct Infrared Imaging.
MALDI-TOF MS – Matrix-Assisted Laser Desorption/Ionization Time-of-Flight Mass Spectrometry.
MNPs – Microplastics.
NaClO – Sodium Hypochlorite.
NaOH – Sodium Hydroxide.
PBS – Phosphate-Buffered Saline.
PE – Polyethylene.
PET – Polyethylene Terephthalate.
PETG – Polyethylene Terephthalate Glycol.
PP – Polypropylene.
PTFE – Polytetrafluoroethylene.
Py-GC/MS – Pyrolysis–Gas Chromatography/Mass Spectrometry.
RT – Room Temperature.
SEM – Scanning Electron Microscopy.
THF – Tetrahydrofuran.
VP-SEM – Variable Pressure Scanning Electron Microscopy *(if cross-referenced)*.
$ZnCl_2$ – Zinc Chloride.

integrative biomedical research exploring tissue-specific accumulation, systemic distribution, and potential associations with disease.

Sample sizes ranged from single autopsy reports [33] to large clinical cohorts [44,54]. Studies with smaller sample numbers often provided higher analytical resolution (e.g., use of SEM, O-PTIR, or MALDI-TOF), whereas those with larger populations tended to adopt standardized, high-throughput techniques such as Py-GC/MS. The ages of the subjects spanned from foetuses (placenta and umbilical cord) to elderly adults (>70 years). Although no direct correlation between age and MNPs load was consistently demonstrated, several reports indicated a trend toward higher MNPs concentrations in adult or chronically ill individuals (e.g., arterial, hepatic, or cerebral tissues), possibly reflecting cumulative exposure or tissue permeability rather than methodological bias. Interestingly, one study reported a significant association not with chronological age, but with *time of death* (2016 vs. 2024), showing a temporal increase in MNPs burden in both liver and brain samples [44].

Among the variables influencing MNPs distribution, tissue type appears to play a major role. Higher concentrations were generally reported in vascular and lipid-rich matrices such as placenta, liver, brain, and atheromatous plaques [23,31,35,44], whereas lower values were found in blood and muscle [31,33]. This pattern suggests that polymer load may correlate with lipid density and vascularization, implying that metabolically active or highly perfused tissues might accumulate more MPs. Moreover, patients with chronic diseases—such as Crohn's disease, cancer, or atherosclerosis—tended to show higher MNPs concentrations compared to controls [24,31,34]. Although causality cannot be inferred, chronic inflammation and endothelial dysfunction may enhance MNPs retention; alternatively, differences in chemical digestion strength applied to diseased tissues might partially explain such variations.

Preventing contamination during sampling and analysis remains one of the greatest methodological challenges in MNPs research. Despite a growing trend toward standardization, no universally accepted protocol for human tissue analysis currently exists. Most studies attempted to minimize external contamination through plastic-free workflows, employing glass or stainless-steel tools, cotton laboratory garments, filtered reagents, and clean-air environments such as laminar flow cabinets or ISO-class clean rooms. These practices mark a clear methodological improvement over earlier studies and reflect increased awareness of laboratory-derived contamination.

However, substantial inter-study variability persists. Some authors described detailed, multi-level blank and control testing, while others provided only partial information or omitted environmental monitoring entirely. Potential contamination sources—such as polyethylene cutting boards, plastic storage containers, or polymer-based consumables—were explicitly acknowledged only in a minority of studies. Notably, those reporting plastic-free protocols, laminar flow workspaces, or environmental control [34,39,40] documented the lowest blank levels (<1 particle or none detected), whereas studies lacking such controls [45,47] tended to report higher MNPs concentrations, likely representing overestimations.

This variability in contamination prevention limits comparability across studies and introduces uncertainty into quantitative results.

Table 4
Detection and analytical techniques used for microplastic identification in human tissues.

Author	Detection Technique	**Brief Description of Method**
Cui, 2025 [31]	Pyrolysis–GC/MS	Thermal degradation at 600 °C under helium; polymer fragments identified via EI-MS (m/z 29–500) using RTX-5 ms column.
Codrington, 2024 [32]	Laser Direct Infrared (LD-IR) & SEM	LDIR chemical imaging (Agilent 8700, Clarity software) for spectral mapping; SEM (Zeiss Merlin) for particle morphology.
Dzierżyński, 2025 [33]	SEM–EDS & O-PTIR	Combined optical, SEM–EDS, and optical photothermal IR microscopy for composition and morphology; DLS and MALDI-TOF MS for particle size and mass spectra.
Wu, 2025 [34]	Laser Direct Infrared (LD-IR)	LDIR (Agilent 8700) spectral scanning, 20–500 μm range, automated particle recognition (~300–400 particles h^{-1}).
Garcia, 2024 [35]	Fluorescence Microscopy, ATR-FTIR & Py-GC/MS	Nile Red fluorescence (LOD ~0.5 μm); ATR-FTIR (>60 % spectral match); Py-GC/MS for polymer quantification with blanks and standards.
Hu, 2024 [36]	Pyrolysis–GC/MS	Polymer identification and quantification by Py-GC–MS; no imaging method applied.
Zhang, 2025 [37]	Raman Microspectroscopy	Confocal Raman (785 nm laser, 0.25 μm resolution); spectral library validation for 0.5–20 μm particles.
Wang, 2025 [38]	Laser Direct Infrared (LD-IR)	LDIR analysis in 900–1800 cm^{-1} range; polymer identification threshold match > 0.65.
Wanderley Lopes de Oliveira, 2025 [39]	Micro-Raman Spectroscopy	Raman spectra (200–3200 cm^{-1}); 10 × 5 s scans per particle; total analyzed area ~ 4 cm^2.
Sun, 2024 [40]	Laser Direct Infrared (LD-IR)	LDIR imaging (20–500 μm detection); polymer identification based on > 80 % spectral match.
Pan, 2025 [41]	Laser Direct Infrared (LD-IR) & SEM	LDIR (Agilent 8700, 20–500 μm, > 0.65 match) combined with SEM for morphology verification.
Guo, 2024 [42]	Py-GC/MS, LD-IR & SEM	Py-GC/MS for polymer ID and quantification; LD-IR (20–500 μm, > 0.65 match); SEM for surface characterization.
Yang, 2025 [43]	Laser Direct Infrared (LD-IR) & SEM	LDIR (20–500 μm, > 0.65 match) with SEM confirmation for morphology and size assessment.
Nihart, 2024 [44]	Pyrolysis–GC/MS	Polymer quantification (μg/g) via Py-GC/MS; cross-year comparison between 2016 and 2024 datasets.
Zhu, 2023 [45]	Laser direct infrared (LD-IR) method	LD-IR acquiring spectra in the 900–1800 cm^{-1} range. Spectra determined against reference libraries with a mapping ratio >90 %
Amereh, 2022 [46]	Digital Microscopy (220X) and Raman microspectroscopy (785 nm laser diode)	Analyzed with Raman XploRA system, with spectra processed using polynomial baseline correction and vector normalization, and matched against the SLOPP Library and KnowItAll software.
Ragusa, 2022 [47]	VP-SEM-dEDS	SEM provides high-resolution imaging and EDS for quantitative chemical composition and elemental mapping analysis.
Ragusa, 2021 [48]	Raman microspectroscopy and VP-SEM-dEDS	Initial inspection with a visible light microscope (× 10 and × 100 objectives), followed by Raman analysis. Spectra compared with the SLOPP Library and KnowItAll software. Also used VP-SEM-dEDS for detailed analysis, similar to Ragusa 2022.
Braun, 2021 [18]	FTIR spectroscopy	Performed with a Perkin Elmer Frontier MIR/FIR Spectrometer, recording infrared spectra in transmission mode and analyzed using SpectrumIMAGE™ software against an in-house library of ten common plastics.
Chen, 2022 [49]	Stereo microscope, μ-FTIR, and Raman spectroscopy	Items larger than 20 μm examined with a Carl Zeiss Stereo microscope and photographed. Spectra matched with a modified database requiring a matching index of ≥ 70 % according to combined libraries of "HR Hummel Polymer and Additives."
Jenner, 2022 [50]	μ-FTIR spectroscopy	Tissue sample Anodisc filters analyzed on ThermoScientific Omnic Picta Nicolet iN10 platform. Dimensions and shapes of particles recorded and categorized.
Amato-Lourenço, 2021 [22]	Light microscopy (× 10 and × 100 objectives) and Raman spectroscopy (633 nm laser)	Inspected filter membranes and obtained Raman spectra. Particle sizes calculated using Image-Pro Plus software, with synthetic polymer particles and fibers observed in autopsy samples.
Ibrahim, 2021 [24]	Optical microscopy, SEM/EDX, and μ-FTIR spectroscopy	Captured micrographs using STEMI2000-c and ScopePad500 cameras, studied surface morphology with SEM/EDX, and identified polymer composition using a Bruker LUMOS micro-FTIR microscope.
Horvatits, 2021 [23]	Fluorescence microscopy	Examined Anodisc and silver filters, counted particles, measured dimensions, recorded shapes, and recalculated concentrations based on initial tissue weight.
Rotchell, 2023 [25]	μ-FTIR spectroscopy	Analyzed Anodisc filters with a Nicolet iN10 μFTIR spectrometer, recording particle dimensions and categorizing shapes using ThermoScientific Omnic Picta Nicolet iN10 software.
Li, 2024 [26]	FTIR and Raman spectroscopy	FTIR spectra obtained in transmittance mode and analyzed with OMNIC 9 software. Particles smaller than 20 μm analyzed with Raman spectroscopy, with

(*continued on next page*)

Table 4 (*continued*)

Author	Detection Technique	**Brief Description of Method**
		spectra processed to identify characteristic wavelengths.

Notes - abbreviations.
FTIR = Fourier-transform infrared spectroscopy;.
Raman = Raman microspectroscopy;.
LD-IR = laser direct infrared imaging;.
SEM = scanning electron microscopy;.
Py-GC/MS = pyrolysis–gas chromatography/mass spectrometry;.

Reported concentrations should therefore be interpreted with caution, particularly when absolute particle counts are used to infer tissue accumulation. Establishing standardized, validated sampling and handling protocols—supported by inter-laboratory calibration and certified reference materials—remains a crucial next step toward reliable and reproducible biomonitoring of MNPs in humans.

The reviewed studies confirm pronounced heterogeneity in extraction and analytical protocols, reflecting both tissue diversity and the absence of standardized methodologies. Although most investigations relied on alkaline or oxidative digestion, the reagents, incubation times, and filtration systems varied substantially, with limited validation of their effects on polymer stability or recovery efficiency. Alkaline (KOH) or oxidative (H_2O_2, HNO_3) digestions may partially degrade sensitive polymers such as polyamide or polyurethane, whereas enzymatic approaches [22,31] better preserve particle morphology and are therefore more suitable for morphological characterization. A general pattern emerges: oxidative methods yield higher MNPs counts but risk polymer degradation, while enzymatic methods provide fewer but more reliable identifications.

A particularly noteworthy methodological advancement was reported by one study [23], which conducted a comprehensive in-house validation of its digestion protocol by exposing fragments (0.2–1 mm) of ten polymers (PE, PP, PVC, PS, PET, PA, PUR, PC, PMMA, and POM) to chemical oxidation and subsequently assessing morphology, weight, and infrared spectra. This internal control ensured polymer integrity and spectral detectability, providing a level of validation rarely achieved elsewhere. The absence of similar internal tests across most studies represents a major methodological weakness, as uncontrolled polymer degradation or loss during digestion may lead to underestimation or misidentification.

Future research should integrate polymer-specific stability testing and recovery experiments into standard workflows. Such “benchmark validation” procedures would enable calibration of digestion strength to polymer resilience and promote inter-laboratory harmonization.

Moving forward, integrating polymer-specific stability testing and recovery experiments into microplastic extraction workflows should become standard practice. This would allow laboratories to calibrate digestion strength to the resilience of target polymers, while also enabling cross-study data harmonization. Establishing such “benchmark validation” procedures would markedly enhance analytical reliability and could serve as a foundational step toward inter-laboratory standardization in human microplastic biomonitoring.

The presence and type of blanks are critical indicators of data reliability. Only a few investigations, mainly published after 2023, systematically implemented multi-blank controls (air, reagent, solution, and instrumental). Studies incorporating these controls and post-analytical corrections [26,50] generally reported lower and more realistic MNPs concentrations. In contrast, the absence of blanks or incomplete reporting often resulted in apparent overestimations. Although two studies specifically employed procedural blanks or negative controls to verify the absence of environmental contamination during collection and processing [18,48], broader adoption of parallel negative controls remains strongly recommended.

Cross-contamination during sampling or treatment remains one of

Table 5
Quality control measures for microplastic detection, including procedural blanks and negative controls.

Author (Year)	**Technique for MNPs detection**	**Procedural Blanks / Negative Controls**
Cui (2025)[31]	Pyrolysis–GC/MS	Field and procedural blanks; commercial MNPs standards; laminar flow hood; verification of contamination absence using ultrapure water–rinsed instruments.
Codrington (2024)[32]	LD-IR & SEM	Procedural blanks included; all reagents filtered; glassware preheated at 250 °C for 8 h to remove residues.
Dzierżyński (2025)[33]	SEM–EDS, O-PTIR	Procedural blanks and parallel controls analyzed under identical conditions.
Wu (2025)[34]	LD-IR	Blank controls using Milli-Q water—confirmed absence of MPs.
Garcia (2024) [35]	Fluorescence microscopy, ATR-FTIR, Py-GC/MS	Blanks run in parallel; ultracentrifuge tubes and cryovials tested for polymer background before use.
Zhang (2025) [37]	Raman microspectroscopy	Procedural blanks and environmental controls in ISO Class 5 clean environment.
Wang (2025)	LD-IR	Milli-Q and blank controls analyzed—no contamination detected.
Wanderley Lopes de Oliveira (2025)	Micro-Raman	Procedural blanks for air, Milli-Q, PBS, and KOH; airborne MNPs detected in controls were excluded from analysis.
Sun (2024)	LD-IR	Procedural and air blanks used; confirmed absence of contamination.
Pan (2025)	LD-IR & SEM	Procedural blanks for reagents, solvents, and laboratory environment; external QC plan applied.
Guo (2024)	Py-GC/MS, LD-IR, SEM	Procedural blanks with Milli-Q water; recovery 81.6–117.4 %.
Zhu (2023)	LD-IR	Plastic-free protocol; no plastic equipment; contamination controls implicitly included. *(Procedural blanks not explicitly stated but implied by protocol.)*
Amereh (2022)	Raman microspectroscopy	Plastic-free protocol; no blanks explicitly mentioned but extensive contamination prevention reported.
Ragusa (2021)	Raman microspectroscopy & VP-SEM-dEDS	Procedural blanks used to monitor and correct contamination.
Braun (2021)	FTIR	Negative and contamination controls applied; materials rinsed with ultrapure water and covered with aluminum foil.
Jenner, 2022	μFTIR spectroscopy	Procedural blanks ($n = 4$) prepared in parallel, mimicking full tissue digestion steps but without lung tissue. Laboratory blanks ($n = 13$) exposed during μFTIR analysis to capture airborne contamination. Results from both blank types combined for correction (subtraction and LOD/LOQ adjustments applied). Results corrected for MNPS contamination.
Amato-Lourenço (2021)	Light microscopy & Raman spectroscopy	Procedural blanks and control samples (from stillborns) used to assess environmental contamination.

(*continued on next page*)

Table 5 (*continued*)

Author (Year)	Technique for MNPs detection	Procedural Blanks / Negative Controls
Horvatits (2021)	Fluorescence microscopy	Blank samples analyzed to assess contamination during processing.
Rotchell (2023)	μFTIR; stereomicroscopy	Procedural blanks processed in parallel to tissue samples
Li (2024)	FTIR and Raman spectroscopy	Procedural blanks (triplicate, using same H_2O_2 solution) performed to correct for solution and procedural background. Additional blank membranes exposed to air for airborne contamination control. All blanks analyzed to verify contamination-free conditions.

Notes: The table summarizes the contamination control strategies adopted in each study, specifying whether procedural blanks, negative controls, or other validation measures were implemented to ensure data reliability.
Abbreviations:.
ATR-FTIR – Attenuated Total Reflectance Fourier-Transform Infrared Spectroscopy.
EDS – Energy Dispersive X-ray Spectroscopy.
FTIR – Fourier-Transform Infrared Spectroscopy.
GC/MS – Gas Chromatography–Mass Spectrometry.
KOH – Potassium Hydroxide.
LD-IR – Laser Direct Infrared Imaging.
LOQ – Limit of Quantification.
LOD – Limit of Detection.
MNPs – Microplastics.
PBS – Phosphate-Buffered Saline.
PMMA – Polymethyl Methacrylate *(if mentioned elsewhere in the same table, optional)*.
Py-GC/MS – Pyrolysis Gas Chromatography–Mass Spectrometry.
SEM – Scanning Electron Microscopy.
VP-SEM-dEDS – Variable Pressure Scanning Electron Microscopy with Dispersive Energy Spectroscopy Detection.
μFTIR – Micro-Fourier-Transform Infrared Spectroscopy.
O-PTIR – Optical Photothermal Infrared Spectroscopy.
QC – Quality Control.

the main obstacles to interpreting truly positive samples, as obtaining completely negative blanks remains difficult. Some authors mitigated this by performing procedures in controlled environments, acknowledging that airborne particles can represent a substantial contamination source.

Characterization of MNPs in human tissues relies primarily on spectroscopic methods, including Raman and Fourier-transform infrared (FTIR) spectroscopy [55–57]. Conventional FTIR is widely used for polymer identification, while micro-FTIR enables the localization of smaller particles on filters [56,58] . Raman spectroscopy offers superior spatial resolution, detecting particles as small as 1 μm, and provides enhanced identification of aromatic compounds [59]. The combination of Raman and FTIR techniques is therefore considered complementary, allowing comprehensive chemical characterization. However, Raman spectra of weathered MNPs often differ from reference libraries, requiring baseline correction, vector normalization, and expert interpretation—factors that currently hinder automation and reproducibility.

Few studies combined multiple analytical methods [33,41] yet such approaches consistently produced more complete and coherent datasets. Instrument sensitivity strongly influences detected concentrations: while Py-GC/MS yields higher mass-based quantification, it lacks morphological information; in contrast, μFTIR and Raman provide detailed polymer identification at the expense of volumetric representativeness.

Quantitative reporting also remains inconsistent. Some studies express MNPs abundance as total fragments per gram of tissue, others extrapolate to the entire organ. Given tissue heterogeneity, reporting

Table 6
Summary of polymer composition, microplastic abundance, and additional characteristics reported across studies.

Author	Polymer Composition (Qualitative)	Microplastic Abundance	Additional Reported Characteristics
Cui, 2025 [31]	PE, PP, PVC, SBR, PMMA, PET, PS, PA6, PA66, PC, PU, ABS	Blood: 75.2 μg/g (12.1–303.2); Plaques: 432.9 μg/g (131.4–1718.8)	Predominant MPs: PE (blood), PP (plaques); intra-/inter-matrix correlations with lipid biomarkers
Codrington, 2024 [32]	PET, PP, PMMA, others (7 polymers total)	Reported as % composition and particle counts; 84 % between 20 and 100 μm	SEM identified additional MNPs (2–20 μm); elongated fibers >100 μm observed
Dzierżyński, 2025 [33]	NB, PAN, PC, PET, PLA, PI, PVC, PS, RE, CE, VT	Not quantified per gram; DLS distributions by organ (200–2400 nm)	Semi-synthetic polymers (cellulose, viscose) ubiquitous; PS–Ag and PET/PAN oligomers tissue-specific
Wu, 2025 [34]	CPE, ACR, Fluororubber, PE (12 total)	1.41–8.59 particles/g depending on tissue	MNPs < 50 μm predominant; fragment morphology; strong correlation with fibrosis severity
Garcia, 2024 [35]	PE (~54 % dominant)	Py-GC/MS: 6.5–685 μg/g (mean 126.8 μg/g)	Procedural blanks and polymer standards confirmed minimal contamination
Hu, 2024 [36]	PE, ABS, N66, PVC, PU, N6, PP, SBR, PET, PMMA, PC	161.22–695.94 μg/g (mean 328.44 μg/g)	PE most abundant (~35 %); inverse correlation of PC/ABS with sperm count
Zhang, 2025 [37]	PS, PTFE, PE, PC	Relative abundance only (% composition); no number/g reported	Combined Raman and Py-GC/MS improved polymer identification (beyond fluorescence limits)
Wang, 2025 [38]	PE, PP, PVC, PA, PMMA, POM, PU, PS, PC	Mean 6.42 particles/g (CT: 7.43; ANT: 5.07)	20–50 μm particles dominant; 94 % detection rate in CT tissues
Wanderley Lopes de Oliveira, 2025 [39]	Placenta: PE, PU, PA, PEVA, PP, PS; Cord: PE, PA, PEVA, PP, PU, PES	Placenta ≈ 0.275 MPs/g; Cord ≈ 0.533 MPs/g	Mostly irregular morphology; transparent color; additives in ~36 % of MPs
Sun, 2024 [40]	PA, PU, PET, CPE, PE, PMMA, ACR, PP, FKM, PS, PVC, BR	Placenta 4.68; Cord 10.40; Membrane 6.56 MPs/g	Dominant polymer = PA; MNPs 20–100 μm; no correlation with maternal age or BMI
Pan, 2025 [41]	PVC, PE, PET, PP, PS	Relative increase in tumor > adjacent tissue (not per gram)	PVC concentration correlated with takeout food frequency and tumor biomarkers
Guo, 2024 [42]	PE, PS, PVC, PA66, PP, FKM, PU, CPE, PET, PIB, ACR, EVA	≈ 19.72 particles/g (12.27–28.44 range)	MNPs 20–50 μm; fibrous/fragmented; strong polymer–polymer and polymer–platelet correlations
Yang, 2025 [43]	PP, EVA, PS, PU, PET, PC, PA, PBS, PHA	Bone 22.9; Cartilage 26.4; Disc 61.1 particles/g	Fragments dominant; distinct polymer sets per tissue; no correlation with age or lifestyle

(*continued on next page*)

Table 6 (*continued*)

Author	Polymer Composition (Qualitative)	Microplastic Abundance	Additional Reported Characteristics
Nihart, 2024 [44]	N/R; polymers confirmed by Py-GC/MS	Liver 465 μg/g; Kidney 666 μg/g; Brain 4763 μg/g (up to 47,730 μg/g in dementia)	MNPS load ↑ in 2024 vs 2016; strongest accumulation in brain; only time of death correlated
Zhu, 2023 [45]	PVC, PP, PBS, PET, PC, PS, PA, Polyester fiber, PE, PAM, PSF	2.70 ± 2.65 particles/g (0.28–9.55 range)	PVC and PP most prevalent (detected in 64.7 % and 58.8 % samples); fragments dominant (67.3 %), fibers (22.2 %); size 20–307 μm (80 % 20–100 μm); no correlation with age or particle size; PVC linked to potential hepatotoxic and reproductive risks
Amereh, 2022 [46]	PE (67.7 %), PS (33.3 %) in normal group; PE (43 %), PS (36.4 %), PET (14.9 %), PP (5.6 %) in IUGR; HDPE and LDPE forms identified	N/R	Up to 3 polymer types/sample; MNPs 12.39 × higher in bottled water users, 4.7 × higher in takeaway food consumers | PE dominated plastic fragments (55–60 %);
Ragusa, 2022 [47]	N/R	% positive: 13 % (normal), 39 % (IUGR)	Higher load in bottled-water consumers; MNPs localized in maternal/fetal sides
Ragusa, 2021 [48]	PP, paint/coating/dye MNPs (pigment-based: Iron hydroxide oxide yellow, Phthalocyanine blue, Violanthrone, Oxo (oxoferriooxy)iron red, Direct Blue 80, Ultramarine Blue, Novoperm Bordeaux HF3R	12 particles detected in 4 placentas	MNPs in all placental villi compartments; ultrastructural organelle alterations
Braun, 2021 [18]	PE, PP, PU, PS	Qualitative (2 MNPs in 4 placentas)	MNPs localized across placental regions; fragments 5–10 μm
Chen, 2022 [49]	PP (core), PS (control)	Not quantified	No MNPs detected after washing; procedural contamination detected
Jenner, 2022 [50]	PP, PET, PE, PE/PP, PS, PTFE, PVA, resin	0.69 ± 0.84 MP/g (adjusted; range 0–8 MPs/sample)	39 MNPs in 11/13 lung samples; detected in all lung regions. Highest abundance in lower region (1.65 ± 0.88 MP/g), > middle (0.33 ± 0.37) > upper (0.23 ± 0.28) ($p < 0.05$). PP detected above LOQ (1.94 MP/g). Shapes: fibers, fragments, films; mean length 223 μm.
Amato-Lourenço, 2021 [22]	PP, PE, PVC, PS, PUR, PA, PE-PP, PS-PVC, CA	31 particles in 13/20 decedents; no MNPs in stillborn controls	Mean particle size 3.92 μm; fibers 11.23 μm. Shapes: fragments (87.5 %), fibers (12.5 %). Dominant polymers: PP, PE. MNPs showed weathering features per Raman spectra. Background contamination minimal (1 PP particle in blanks). Greater load in lower lung region
Ibrahim, 2021 [24]	PC, PA, PP	28.1 ± 15.4 particles/g	MNPs 3.9 μm; fibers ~11 μm; one PP particle in blanks
Horvatits, 2021 [23]	PS, PVC, PET, PMMA, POM, PP	1.4 particles/g (1.2 corrected)	96 % filamentous, transparent fibers ~1.1 mm long
Rotchell, 2023 [25]	PVAc, nylon/EVA, PVAE, PUR	14.99 ± 17.18 MPs/g (blank-corrected)	Lowest MNPs concentrations in kidney samples. Non-MNPs additives (e.g., propylene glycol dilaurate, Span 40, epoxidized soybean oil) also observed.
Li, 2024 [26]	PET, PE, RA, PES, PP, PA, PVC, PS, PC	5.24 ± 2.07 MPs/g (1.16–10.77 range)	MNPs smaller but more abundant in hip than knee ($p < 0.01$). Size 11–151 μm (mean ≈ 50 μm). Predominant colors blue, transparent, white. Same polymers in hip and knee, suggesting shared exposure route.

Notes: The table compiles qualitative and quantitative findings on polymer types, microplastic concentrations, and relevant morphological or biological correlations as described by each author. Units and reporting formats are presented as stated in the original studies.

Abbreviations:.

N/R: Not reported in the original publication. Despite attempts to contact the corresponding authors, the missing information could not be retrieved and is therefore reported as a limitation of the available evidence. MNPs = Microplastics.

PE = Polyethylene;
PP = Polypropylene;
PVC = Polyvinyl Chloride;
PS = Polystyrene;
PET = Polyethylene Terephthalate;
PU = Polyurethane;
PA = Polyamide (Nylon);
PA6 = Polyamide 6;
PA66 = Polyamide 66;
PMMA = Polymethyl Methacrylate;
PC = Polycarbonate;
ABS = Acrylonitrile Butadiene Styrene;
SBR = Styrene-Butadiene Rubber;
CPE = Chlorinated Polyethylene;
ACR = Acrylic Resin;
FKM = Fluoroelastomer (Fluorocarbon Rubber);
PI = Polyimide;
PLA = Polylactic Acid;
PAN = Polyacrylonitrile;
POM = Polyoxymethylene;
EVA = Ethylene Vinyl Acetate;
PEVA = Polyethylene Vinyl Acetate;
PBS = Polybutylene Succinate;

PHA = Polyhydroxyalkanoate;
PTFE = Polytetrafluoroethylene (Teflon);
PIB = Polyisobutylene;
RE = Resin;
CE = Cellulose;
VT = Viscose (Regenerated Cellulose);
NB = Nitrile Butadiene Rubber;
BR = Butadiene Rubber;
CF = Colonic Fibrosis;
CD-MAT = Crohn's Disease – Mesenteric Adipose Tissue;
uIleum = Unstructured Ileum;
iIleum = Inflamed Ileum;
CT = Corpus Tissue;
ANT = Anterior Tissue;
μg/g = Micrograms of MNPs per gram of tissue;.

MNPs counts per gram of processed tissue before digestion provides the most reproducible metric. Spatial variability within a single organ has also been documented—for example, Li et al. observed differences between hip and knee tissues [26], and Jenner et al. reported higher MNPs concentrations at the lung bases [50].

FTIR spectroscopy currently represents the most widely used technique for routine MNPs analysis in environmental research, although its application to biological matrices remains comparatively limited. FTIR is a powerful diagnostic tool for polymer characterization, capable of identifying specific vibrational bonds characteristic of different plastics [58,60]. Its major strengths lie in its robustness, accessibility, and ability to provide semi-quantitative information on polymer type and abundance. Furthermore, the recent development of automated FTIR mapping and imaging systems has enhanced its potential for high-throughput analysis in complex biological samples [54]. Raman spectroscopy, on the other hand, has gained increasing adoption for MNPs detection in biological specimens and offers several advantages over FTIR. A key benefit is its superior spatial resolution, which enables the identification of particles as small as 1 μm, whereas conventional FTIR methods typically cannot reliably detect MNPs smaller than 10 μm within internal tissues. In addition, Raman spectroscopy excels in identifying polymers containing aromatic or conjugated bonds, which FTIR may underrepresent due to weaker absorbance in these regions. This complementarity makes the combination of FTIR and Raman spectroscopy particularly powerful, providing a more comprehensive and reliable chemical characterization of MNPs [54].

Polymer identification by Raman spectroscopy relies on spectral matching between sample spectra and established reference libraries. However, a major analytical challenge arises from the weathering of MNPs in vivo, which alters their chemical structure and consequently their spectral profiles. Aged or oxidized particles often display weakened or missing characteristic peaks, complicating identification and leading to potential misclassification. To address this issue, several reference databases containing Raman spectra of weathered MNPs have been developed. Moreover, raw Raman spectra typically undergo preprocessing steps—such as baseline correction and vector normalization—to reduce noise and improve spectral quality. Nonetheless, spectral matching accuracy still depends on the operator's expertise and the quality of the reference library. Literature reports indicate that spectral concordance above 70 % is generally accepted for confident identification [23], although lower values have occasionally been tolerated when supported by morphological and contextual evidence.

Despite its diagnostic precision, Raman spectroscopy remains time-consuming, as each spectrum must be collected individually. This limitation, combined with its susceptibility to fluorescence interference, hinders its large-scale application for routine biomonitoring. Consequently, both Raman and FTIR approaches are often applied selectively to representative subsamples. The identification of polymeric fibers through visual inspection alone remains highly unreliable: visual sorting can yield error rates up to 70 %, particularly for smaller particles, underscoring the need for spectroscopic confirmation [61]. Beyond FTIR and Raman spectroscopy, several alternative or complementary techniques have been explored. These include laser direct infrared (LDIR) analysis, which combines IR imaging with automation for particle mapping; scanning or transmission electron microscopy for morphological assessment; and fluorescence microscopy, particularly for stained or autofluorescent MPs. However, these approaches remain largely supplementary due to limitations in polymer specificity or throughput.

Across studies, the most frequently detected polymers were polyethylene (PE), polypropylene (PP) and polyvinyl chloride (PVC)—a distribution consistent with global plastic production and environmental prevalence. However, tissue-specific polymer patterns emerged. In placental and blood samples, PE and PP predominated, suggesting primary exposure through dietary or airborne routes. In contrast, tumour and neural tissues showed a higher incidence of technical polymers such as polyurethane (PU), polymethyl methacrylate (PMMA), and polyoxymethylene (POM), possibly reflecting occupational or medical sources of exposure. This variability supports the hypothesis that polymer composition reflects exposure source and pathway rather than analytical bias.

Overall, compiled evidence reveals marked inter-study heterogeneity in both MNPs abundance and polymeric composition, influenced by matrix type, analytical sensitivity, and regional exposure context. While most studies identified PE, PP, and PVC as dominant, certain investigations—particularly those on reproductive tissues—reported polytetrafluoroethylene (PTFE) or polyamide (PA) as prevalent types, possibly indicating tissue-specific retention or distinct exposure routes. Studies employing comprehensive analytical workflows—such as combined Raman and Py-GC/MS—consistently detected a broader range of polymers than single-method approaches, underscoring the importance of multi-analytical validation. Some authors incorporated procedural blanks or polymer standards to verify data reliability, yet such practices remain inconsistently implemented. These methodological disparities continue to impede direct cross-study comparison and hinder precise estimation of human MNPS burden.

Regardless the technique used to identify MPs, how to express quantitative results is still debated. No consensus currently exists on how to express MNPs abundance, leading to inconsistencies in reported units and metrics. Some studies report the number of particles per gram of analysed tissue, whereas others extrapolate total particle counts to entire organs. Given the heterogeneity of MNPs distribution within tissues, expressing results as *particles per gram of pre-weighed tissue* represents the most standardized and reproducible approach. Spatial heterogeneity has also been observed within the same tissue—Li et al. found differing MNPs concentrations between hip and knee samples [26], and Jenner et al. reported higher loads at the lung bases [50] —highlighting the need for sampling standardization and replication within organs.

Reported MNPs concentrations vary by several orders of magnitude (from <1 to thousands of μg g^{-1}), but these differences likely reflect methodological variability more than true biological variation. Techniques such as Py-GC/MS tend to yield higher values due to their mass-based detection, while optical or spectroscopic counting approaches produce lower but more particle-specific estimates. Notably, a temporal trend is emerging: studies published after 2023 generally report lower MNPs concentrations, likely owing to improved contamination control and adoption of standardized blank correction protocols.

Recent investigations have increasingly integrated morphometric and dimensional analyses, showing that fragments smaller than 100 μm are the most prevalent, often transparent or white in color. Several

authors [31,34,42] have also attempted to correlate biological parameters—such as lipid content, inflammation, or fibrosis—with MNPs load. Although no causal relationship has yet been demonstrated, these observations open new avenues for clinical and mechanistic research. Nevertheless, the lack of standardized data reporting continues to limit inter-study comparability and meta-analytic synthesis.

The potential health implications of MNPs accumulation in human tissues remain largely uncertain due to limited experimental evidence. In vitro studies using human cell lines—particularly those exposed to polystyrene particles—have demonstrated cytotoxic and pro-inflammatory effects, especially at higher concentrations and with smaller particle sizes. MNPs can induce local immune activation through macrophage or epithelial cell responses and may trigger oxidative stress, apoptosis, or metabolic dysregulation.

The small size and hydrophobicity of MNPs confer a large reactive surface area that favours the adsorption and transport of microorganisms [62,63], including antibiotic-resistant bacteria and genes as well as persistent contaminants such as PFAS. Thus, MNPs may act as vectors facilitating the entry of these co-contaminants into biological systems. Experimental and epidemiological evidence further associates MNPs exposure with oxidative stress [64], inflammation [65], endocrine disruption, impaired reproductive function [66,67], reduced immune response [68], and alterations in lipid and energy metabolism [30]. Given these emerging toxicological concerns, the systematic analysis of MNPs in human tissues warrants careful methodological standardization and rigorous contamination control. Establishing harmonized analytical pipelines—from sampling to polymer identification—will be essential to accurately assess exposure levels, evaluate biological effects, and support risk assessment frameworks for human health.

This review is limited by the marked heterogeneity of analytical protocols and reporting units across studies, which hampers direct data comparison. The inconsistent implementation of procedural blanks and contamination controls also introduces uncertainty regarding the true endogenous presence of microplastics in human tissues. Moreover, most available studies remain descriptive, preventing causal inference or reliable estimation of exposure–effect relationships. Standardized, validated methodologies and harmonized reporting frameworks are therefore essential to enhance the reliability and comparability of future findings.

5. Conclusion

This systematic review confirms the widespread detection of MNPs across diverse human solid tissues, with polyethylene, polypropylene, and polyvinyl chloride consistently emerging as the dominant polymers. Tissue-specific differences in polymer composition were also observed, with a higher relative occurrence of technical polymers in specific pathological tissues, suggesting that polymer profiles may reflect exposure source and tissue context. However, substantial heterogeneity in analytical protocols, detection techniques, and reporting units continues to impede cross-study comparability and the accurate estimation of human tissue burden. Despite notable methodological progress—such as the adoption of plastic-free workflows, systematic use of procedural blanks, and the integration of complementary spectroscopic and thermochemical analyses—no standardized protocol yet exists for tissue collection, polymer extraction, or quantitative assessment.

Recent methodological refinements, particularly in contamination control and quality assurance, appear to have reduced previous overestimations of MNPs abundance, highlighting an ongoing shift toward greater analytical rigor. The predominance of sub-100 μm fragments and preliminary associations between MNP load and selected pathological or biochemical parameters underscore the urgency of methodological harmonization. The establishment of internationally accepted guidelines spanning tissue acquisition to data interpretation remains essential to enhance data reliability, enable meaningful inter-study comparison, and ultimately clarify the health implications of microplastic accumulation in human tissues.

Statements and declarations

Funding

This publication has been financed with the support by Ministero della Salute 5 × 1000 fund raising campaign 5xmille 2022 of the Rizzoli Orthopaedic Institute;

Ethics approval

This study is a systematic review and did not involve any direct research with human participants or animals. As such, ethics approval was not required.

CRediT authorship contribution statement

Simone Ottavio Zielli: Writing – review & editing, Writing – original draft, Formal analysis, Data curation, Conceptualization. **Jennifer Paola Pascali:** Writing – review & editing, Supervision, Formal analysis, Data curation. **Antonio Mazzotti:** Supervision, Conceptualization. **Paolo Fais:** Writing – review & editing, Supervision, Methodology, Conceptualization. **Milena Fini:** Project administration, Methodology, Funding acquisition. **Cesare Faldini:** Supervision, Project administration. **Susi Pelotti:** Supervision, Resources.

Declaration of competing interest

The authors declare that they have no known competing financial interests or personal relationships that could have appeared to influence the work reported in this paper.

Acknowledgments

This publication has been financed with the support by Ministero della Salute 5 × 1000 fund raising campaign 5xmille 2022 of the Rizzoli Orthopaedic Institute;

Data availability

Data will be made available on request.

References

[1] C.J. Rhodes, Plastic pollution and potential solutions, Sci. Prog. 101 (2018) 207–260, https://doi.org/10.3184/003685018X15294876706211.
[2] E. Winiarska, M. Jutel, M. Zemelka-Wiacek, The potential impact of nano- and microplastics on Human health: understanding Human health risks, Environ. Res. 251 (2024) 118535, https://doi.org/10.1016/j.envres.2024.118535.
[3] A. Collignon, J.-H. Hecq, F. Galgani, F. Collard, A. Goffart, Annual variation in neustonic micro- and meso-plastic particles and zooplankton in the Bay of Calvi (Mediterranean–Corsica), Mar. Pollut. Bull. 79 (2014) 293–298, https://doi.org/10.1016/j.marpolbul.2013.11.023.
[4] M. Filella, Questions of size and numbers in environmental research on microplastics: methodological and conceptual aspects, Environ. Chem. 12 (2015) 527–538, https://doi.org/10.1071/EN15012.
[5] A.L. Andrady, Microplastics in the marine environment, Mar. Pollut. Bull. 62 (2011) 1596–1605, https://doi.org/10.1016/j.marpolbul.2011.05.030.
[6] J.P.G.L. Frias, R. Nash, Microplastics: finding a consensus on the definition, Mar. Pollut. Bull. 138 (2019) 145–147, https://doi.org/10.1016/j.marpolbul.2018.11.022.
[7] A. Cózar, F. Echevarría, J.I. González-Gordillo, X. Irigoien, B. Úbeda, S. Hernández-León, Á.T. Palma, S. Navarro, J. García-de-Lomas, A. Ruiz, et al., Plastic debris in the open ocean, Proceed. National Acad. Sci. 111 (2014) 10239–10244, https://doi.org/10.1073/pnas.1314705111.
[8] M. Filella, Questions of size and numbers in environmental research on microplastics: methodological and conceptual aspects, Environ. Chem. 12 (2015) 527–538, https://doi.org/10.1071/EN15012.
[9] R. Lehner, C. Weder, A. Petri-Fink, B. Rothen-Rutishauser, Emergence of nanoplastic in the environment and possible impact on Human health, Environ. Sci. Technol. 53 (2019) 1748–1765, https://doi.org/10.1021/acs.est.8b05512.

[10] G.J. Palm, L. Reisky, D. Böttcher, H. Müller, E.A.P. Michels, M.C. Walczak, L. Berndt, M.S. Weiss, U.T. Bornscheuer, G. Weber, Structure of the plastic-degrading Ideonella Sakaiensis MHETase bound to a substrate, Nat. Commun. 10 (2019) 1717, https://doi.org/10.1038/s41467-019-09326-3.
[11] D. Luo, X. Chu, Y. Wu, Z. Wang, Z. Liao, X. Ji, J. Ju, B. Yang, Z. Chen, R. Dahlgren, et al., Micro- and nano-plastics in the atmosphere: a review of occurrence, properties and Human health risks, J. Hazard. Mater. 465 (2024) 133412, https://doi.org/10.1016/j.jhazmat.2023.133412.
[12] Y. Arif, A.R. Mir, P. Zieliński, S. Hayat, A. Bajguz, Microplastics and nanoplastics: source, behavior, remediation, and multi-level environmental impact, J. Environ. Manage 356 (2024) 120618, https://doi.org/10.1016/j.jenvman.2024.120618.
[13] Measures to Restrict Microplastics Available online: https://ec.europa.eu/commission/presscorner/detail/en/ip_23_4581 (accessed on 16 October 2024).
[14] Human Consumption of Microplastics | Environmental Science & Technology Available online: https://pubs.acs.org/doi/10.1021/acs.est.9b01517 (accessed on 26 July 2024).
[15] A. Vdovchenko, M. Resmini, Mapping microplastics in humans: analysis of polymer types, and shapes in food and drinking water-A systematic review, Int. J. Mol. Sci. 25 (2024) 7074, https://doi.org/10.3390/ijms25137074.
[16] C.-L. Bai, D. Wang, Y.-L. Luan, S.-N. Huang, L.-Y. Liu, Y. Guo, A review on micro- and nanoplastics in humans: implication for their translocation of barriers and potential health effects, Chemosphere 361 (2024) 142424, https://doi.org/10.1016/j.chemosphere.2024.142424.
[17] J. Xue, Z. Xu, X. Hu, Y. Lu, Y. Zhao, H. Zhang, Microplastics in maternal amniotic fluid and their associations with gestational age, Sci. Total. Environ. 920 (2024) 171044, https://doi.org/10.1016/j.scitotenv.2024.171044.
[18] T. Braun, L. Ehrlich, W. Henrich, S. Koeppel, I. Lomako, P. Schwabl, B. Liebmann, Detection of microplastic in Human placenta and meconium in a clinical setting, Pharmaceutics. 13 (2021) 921, https://doi.org/10.3390/pharmaceutics13070921.
[19] S. Liu, J. Guo, X. Liu, R. Yang, H. Wang, Y. Sun, B. Chen, R. Dong, Detection of various microplastics in placentas, meconium, infant feces, breastmilk and infant formula: a pilot prospective study, Science of The Total Environment 854 (2023) 158699, https://doi.org/10.1016/j.scitotenv.2022.158699.
[20] Y. Zhong, Y. Yang, L. Zhang, D. Ma, K. Wen, J. Cai, Z. Cai, C. Wang, X. Chai, J. Zhong, et al., Revealing new insights: two-center evidence of microplastics in Human vitreous humor and their implications for ocular health, Science of The Total Environment 921 (2024) 171109, https://doi.org/10.1016/j.scitotenv.2024.171109.
[21] D. Zhang, C. Wu, Y. Liu, W. Li, S. Li, L. Peng, L. Kang, S. Ullah, Z. Gong, Z. Li, et al., Microplastics are detected in Human gallstones and have the ability to form large cholesterol-microplastic heteroaggregates, J. Hazard. Mater. 467 (2024) 133631, https://doi.org/10.1016/j.jhazmat.2024.133631.
[22] L.F. Amato-Lourenço, R. Carvalho-Oliveira, G.R. Júnior, L. Dos Santos Galvão, R. A. Ando, T. Mauad, Presence of airborne microplastics in Human lung tissue, J. Hazard. Mater. 416 (2021) 126124, https://doi.org/10.1016/j.jhazmat.2021.126124.
[23] T. Horvatits, M. Tamminga, B. Liu, M. Sebode, A. Carambia, L. Fischer, K. Püschel, S. Huber, E.K. Fischer, Microplastics detected in cirrhotic liver tissue, EBioMedicine 82 (2022) 104147, https://doi.org/10.1016/j.ebiom.2022.104147.
[24] Y.S. Ibrahim, S. Tuan Anuar, A.A. Azmi, W.M.A. Wan Mohd Khalik, S. Lehata, S. R. Hamzah, D. Ismail, Z.F. Ma, A. Dzulkarnaen, Z. Zakaria, et al., Detection of microplastics in Human colectomy specimens, JGH. Open. 5 (2021) 116–121, https://doi.org/10.1002/jgh3.12457.
[25] J.M. Rotchell, L.C. Jenner, E. Chapman, R.T. Bennett, I.O. Bolanle, M. Loubani, L. Sadofsky, T.M. Palmer, Detection of microplastics in Human saphenous vein tissue using μFTIR: a pilot study, PLoS. One 18 (2023) e0280594, https://doi.org/10.1371/journal.pone.0280594.
[26] Z. Li, Y. Zheng, Z. Maimaiti, J. Fu, F. Yang, Z.-Y. Li, Y. Shi, L.-B. Hao, J.-Y. Chen, C. Xu, Identification and analysis of microplastics in Human lower limb joints, J. Hazard. Mater. 461 (2024) 132640, https://doi.org/10.1016/j.jhazmat.2023.132640.
[27] W. Kwon, D. Kim, H.-Y. Kim, S.W. Jeong, S.-G. Lee, H.-C. Kim, Y.-J. Lee, M. K. Kwon, J.-S. Hwang, J.E. Han, et al., Microglial phagocytosis of polystyrene microplastics results in immune alteration and apoptosis in Vitro and in vivo, Sci. Total. Environ. 807 (2022) 150817, https://doi.org/10.1016/j.scitotenv.2021.150817.
[28] Y. Ma, D. Xu, Z. Wan, Z. Wei, Z. Chen, Y. Wang, X. Han, Y. Chen, Exposure to different surface-modified polystyrene nanoparticles caused anxiety, depression, and social deficit in mice via damaging mitochondria in neurons, Science of The Total Environment 919 (2024) 170739, https://doi.org/10.1016/j.scitotenv.2024.170739.
[29] K. Wang, Y. Du, P. Li, C. Guan, M. Zhou, L. Wu, Z. Liu, Z. Huang, Nanoplastics causes heart aging/myocardial cell senescence through the Ca2+/mtDNA/cGAS-STING signaling cascade, J. Nanobiotechnology. 22 (2024) 96, https://doi.org/10.1186/s12951-024-02375-x.
[30] J. Teng, J. Zhao, X. Zhu, E. Shan, Q. Wang, Oxidative stress biomarkers, physiological responses and proteomic profiling in oyster (*Crassostrea Gigas*) exposed to microplastics with irregular-shaped PE and PET microplastic, Science of The Total Environment 786 (2021) 147425, https://doi.org/10.1016/j.scitotenv.2021.147425.
[31] C. Cui, Z. Guo, Y. Liu, N. Han, J. Song, Y. Chen, Y. Zheng, C. Sheng, L. Balmer, H. Li, et al., Tissue-specific distribution of microplastics in Human blood and carotid plaques: a paired sample analysis, Environ. Int. 203 (2025) 109743, https://doi.org/10.1016/j.envint.2025.109743.
[32] J. Codrington, A.A. Varnum, L. Hildebrandt, D. Pröfrock, J. Bidhan, K. Khodamoradi, A.-L. Höhme, M. Held, A. Evans, D. Velasquez, et al., Detection of microplastics in the Human penis, Int. J. Impot. Res. 37 (2025) 377–383, https://doi.org/10.1038/s41443-024-00930-6.
[33] E. Dzierżyński, E. Blicharz-Grabias, I. Komaniecka, R. Panek, A. Forma, P. J. Gawlik, D. Puźniak, W. Flieger, A. Choma, K. Suśniak, et al., Post-mortem evidence of microplastic bioaccumulation in Human organs: insights from advanced imaging and spectroscopic analysis, Arch. Toxicol. 99 (2025) 4051–4066, https://doi.org/10.1007/s00204-025-04092-2.
[34] F. Wu, F. Wu, X. Liu, W. Xie, Y. Liang, Y. Ye, X. Xiao, K. Sun, L. Bai, S. Liu, et al., Microplastic accumulation in fibrotic intestinal tissue and mesenteric adipose tissue in Crohn's Disease patients, Environ. Res. 271 (2025) 121077, https://doi.org/10.1016/j.envres.2025.121077.
[35] M.A. Garcia, R. Liu, A. Nihart, E. El Hayek, E. Castillo, E.R. Barrozo, M.A. Suter, B. Bleske, J. Scott, K. Forsythe, et al., Quantitation and identification of microplastics accumulation in Human placental specimens using pyrolysis gas chromatography mass spectrometry, Toxicological Sciences 199 (2024) 81–88, https://doi.org/10.1093/toxsci/kfae021.
[36] C.J. Hu, M.A. Garcia, A. Nihart, R. Liu, L. Yin, N. Adolphi, D.F. Gallego, H. Kang, M. J. Campen, X. Yu, Microplastic presence in dog and Human testis and its potential association with sperm count and weights of testis and epididymis, Toxicological Sciences 200 (2024) 235–240, https://doi.org/10.1093/toxsci/kfae060.
[37] L. Zhang, J. Tian, X. Zhu, L. Wang, X. Yun, L. Liang, S. Duan, Cross-platform detection of microplastics in Human biological tissues: comparing spectroscopic and chromatographic approaches, J. Hazard. Mater. 492 (2025) 138133, https://doi.org/10.1016/j.jhazmat.2025.138133.
[38] M. Wang, Q. Liu, X. Zhang, H. Jiang, X. Zhang, Identification and analysis of microplastics in Human penile cancer tissues, Science of The Total Environment 969 (2025) 178815, https://doi.org/10.1016/j.scitotenv.2025.178815.
[39] C.W.L. de Oliveira, L.F.A. de Magalhaes Oliveira, J. Garcia, R.B. Weingrill, J. Urschitz, S.T. Souza, E.J.S. Fonseca, S. Ospina-Prieto, A.U. Borbely, First evidence of microplastic accumulation in placentas and umbilical cords from pregnancies in Brazil, An. Acad. Bras. Cienc. 97 (2025) e20241298, https://doi.org/10.1590/0001-3765202520241298.
[40] H. Sun, X. Su, J. Mao, Y. Liu, G. Li, Q. Du, Microplastics in maternal blood, fetal appendages, and umbilical vein blood, Ecotoxicol. Environ. Saf. 287 (2024) 117300, https://doi.org/10.1016/j.ecoenv.2024.117300.
[41] W. Pan, J. Hao, M. Zhang, H. Liu, F. Tian, X. Zhang, Z. Jiang, C. Chen, M. Gao, H. Zhang, Identification and analysis of microplastics in peritumoral and tumor tissues of colorectal cancer, Sci. Rep. 15 (2025) 16130, https://doi.org/10.1038/s41598-025-98268-6.
[42] X. Guo, L. Wang, X. Wang, D. Li, H. Wang, H. Xu, Y. Liu, R. Kang, Q. Chen, L. Zheng, et al., Discovery and analysis of microplastics in Human bone marrow, J. Hazard. Mater. 477 (2024) 135266, https://doi.org/10.1016/j.jhazmat.2024.135266.
[43] Q. Yang, Y. Peng, X. Wu, X. Cao, P. Zhang, Z. Liang, J. Zhang, Y. Zhang, P. Gao, Y. Fu, et al., Microplastics in Human skeletal tissues: presence, distribution and health implications, Environ. Int. 196 (2025) 109316, https://doi.org/10.1016/j.envint.2025.109316.
[44] A.J. Nihart, M.A. Garcia, E. El Hayek, R. Liu, M. Olewine, J.D. Kingston, E. F. Castillo, R.R. Gullapalli, T. Howard, B. Bleske, et al., Bioaccumulation of microplastics in decedent Human brains, Nat. Med. 31 (2025) 1114–1119, https://doi.org/10.1038/s41591-024-03453-1.
[45] L. Zhu, J. Zhu, R. Zuo, Q. Xu, Y. Qian, L. An, Identification of microplastics in Human placenta using laser direct infrared spectroscopy, Science of The Total Environment 856 (2023) 159060, https://doi.org/10.1016/j.scitotenv.2022.159060.
[46] F. Amereh, N. Amjadi, A. Mohseni-Bandpei, S. Isazadeh, Y. Mehrabi, A. Eslami, Z. Naeiji, M. Rafiee, Placental plastics in young women from general population correlate with reduced foetal growth in IUGR pregnancies, Environmental Pollution 314 (2022) 120174, https://doi.org/10.1016/j.envpol.2022.120174.
[47] A. Ragusa, M. Matta, L. Cristiano, R. Matassa, E. Battaglione, A. Svelato, C. De Luca, S. D'Avino, A. Gulotta, M.C.A. Rongioletti, et al., Deeply in plasticenta: presence of microplastics in the intracellular compartment of Human placentas, IJERPH 19 (2022) 11593, https://doi.org/10.3390/ijerph191811593.
[48] A. Ragusa, A. Svelato, C. Santacroce, P. Catalano, V. Notarstefano, O. Carnevali, F. Papa, M.C.A. Rongioletti, F. Baiocco, S. Draghi, et al., Plasticenta: first evidence of microplastics in Human placenta, Environ. Int. 146 (2021) 106274, https://doi.org/10.1016/j.envint.2020.106274.
[49] K. Lu, D. Zhan, Y. Fang, L. Li, G. Chen, S. Chen, L. Wang, Microplastics, potential threat to patients with lung diseases, Front. Toxicol. 4 (2022) 958414, https://doi.org/10.3389/ftox.2022.958414.
[50] L.C. Jenner, J.M. Rotchell, R.T. Bennett, M. Cowen, V. Tentzeris, L.R. Sadofsky, Detection of microplastics in Human lung tissue using μftir spectroscopy, Science of The Total Environment 831 (2022) 154907, https://doi.org/10.1016/j.scitotenv.2022.154907.
[51] L. Zhu, J. Zhu, R. Zuo, Q. Xu, Y. Qian, L. An, Identification of microplastics in Human placenta using laser direct infrared spectroscopy, Science of The Total Environment 856 (2023) 159060, https://doi.org/10.1016/j.scitotenv.2022.159060.
[52] Microplastics are everywhere — We need to understand how they affect Human health, Nat. Med. 30 (2024), https://doi.org/10.1038/s41591-024-02968-x, 913–913.
[53] N. Kumar, M. Lamba, A.K. Pachar, S. Yadav, A. Acharya, Microplastics – A growing concern as carcinogens in cancer etiology: emphasis on biochemical and molecular mechanisms, Cell Biochem. Biophys. (2024), https://doi.org/10.1007/s12013-024-01436-0.

[54] Y. Chen, D. Wen, J. Pei, Y. Fei, D. Ouyang, H. Zhang, Y. Luo, Identification and quantification of microplastics using fourier-transform infrared spectroscopy: current status and future prospects, Curr. Opin. Environ. Sci. Health 18 (2020) 14–19, https://doi.org/10.1016/j.coesh.2020.05.004.
[55] J.-L. Xu, K.V. Thomas, Z. Luo, A.A. Gowen, FTIR and Raman imaging for microplastics analysis: state of the art, challenges and prospects, TrAC Trends in Analytical Chemistry 119 (2019) 115629, https://doi.org/10.1016/j.trac.2019.115629.
[56] W.J. Shim, S.H. Hong, S.E. Eo, Identification methods in Microplastic analysis: a review, Anal. Methods 9 (2017) 1384–1391, https://doi.org/10.1039/C6AY02558G.
[57] H. Luo, Y. Li, Y. Zhao, Y. Xiang, D. He, X. Pan, Effects of accelerated aging on characteristics, leaching, and toxicity of commercial lead chromate pigmented microplastics, Environmental Pollution 257 (2020) 113475, https://doi.org/10.1016/j.envpol.2019.113475.
[58] J.P. Harrison, J.J. Ojeda, M.E. Romero-González, The applicability of reflectance micro-fourier-transform infrared spectroscopy for the detection of synthetic microplastics in marine sediments, Science of The Total Environment 416 (2012) 455–463, https://doi.org/10.1016/j.scitotenv.2011.11.078.
[59] Z. Sobhani, X. Zhang, C. Gibson, R. Naidu, M. Megharaj, C. Fang, Identification and visualisation of microplastics/nanoplastics by Raman Imaging (i): down to 100 nm, Water. Res. 174 (2020) 115658, https://doi.org/10.1016/j.watres.2020.115658.
[60] C.N. Andoh, F. Attiogbe, N.O. Bonsu Ackerson, M. Antwi, K. Adu-Boahen, Fourier transform infrared spectroscopy: an analytical technique for microplastic identification and quantification, Infrared. Phys. Technol. 136 (2024) 105070, https://doi.org/10.1016/j.infrared.2023.105070.
[61] V. Hidalgo-Ruz, L. Gutow, R.C. Thompson, M. Thiel, Microplastics in the marine environment: a review of the methods used for identification and quantification, Environ. Sci. Technol. 46 (2012) 3060–3075, https://doi.org/10.1021/es2031505.
[62] E. Fournier, L. Etienne-Mesmin, C. Grootaert, L. Jelsbak, K. Syberg, S. Blanquet-Diot, M. Mercier-Bonin, Microplastics in the Human digestive environment: a focus on the potential and challenges facing in vitro gut model development, J. Hazard. Mater. 415 (2021) 125632, https://doi.org/10.1016/j.jhazmat.2021.125632.
[63] X. Sun, B. Chen, Q. Li, N. Liu, B. Xia, L. Zhu, K. Qu, Toxicities of polystyrene nano- and microplastics toward marine bacterium *halomonas alkaliphila*, Science of The Total Environment 642 (2018) 1378–1385, https://doi.org/10.1016/j.scitotenv.2018.06.141.
[64] A.A. Babaei, M. Rafiee, F. Khodagholi, E. Ahmadpour, F. Amereh, Nanoplastics-induced oxidative stress, antioxidant defense, and physiological response in exposed Wistar Albino rats, Environ. Sci. Pollut. Res. Int. 29 (2022) 11332–11344, https://doi.org/10.1007/s11356-021-15920-0.
[65] B. Li, Y. Ding, X. Cheng, D. Sheng, Z. Xu, Q. Rong, Y. Wu, H. Zhao, X. Ji, Y. Zhang, Polyethylene microplastics affect the distribution of gut microbiota and inflammation development in mice, Chemosphere 244 (2020) 125492, https://doi.org/10.1016/j.chemosphere.2019.125492.
[66] F. Amereh, M. Babaei, A. Eslami, S. Fazelipour, M. Rafiee, The emerging risk of exposure to nano(Micro)plastics on endocrine disturbance and reproductive toxicity: from a hypothetical scenario to a global public health challenge, Environ. Pollut. 261 (2020) 114158, https://doi.org/10.1016/j.envpol.2020.114158.
[67] J. Hu, X. Qin, J. Zhang, Y. Zhu, W. Zeng, Y. Lin, X. Liu, Polystyrene microplastics disturb maternal-fetal immune balance and cause reproductive toxicity in pregnant mice, Reproductive Toxicology 106 (2021) 42–50, https://doi.org/10.1016/j.reprotox.2021.10.002.
[68] J.-N. Huang, B. Wen, J.-G. Zhu, Y.-S. Zhang, J.-Z. Gao, Z.-Z. Chen, Exposure to microplastics impairs digestive performance, stimulates immune response and induces microbiota dysbiosis in the gut of juvenile guppy (Poecilia Reticulata), Sci. Total. Environ. 733 (2020) 138929, https://doi.org/10.1016/j.scitotenv.2020.138929.